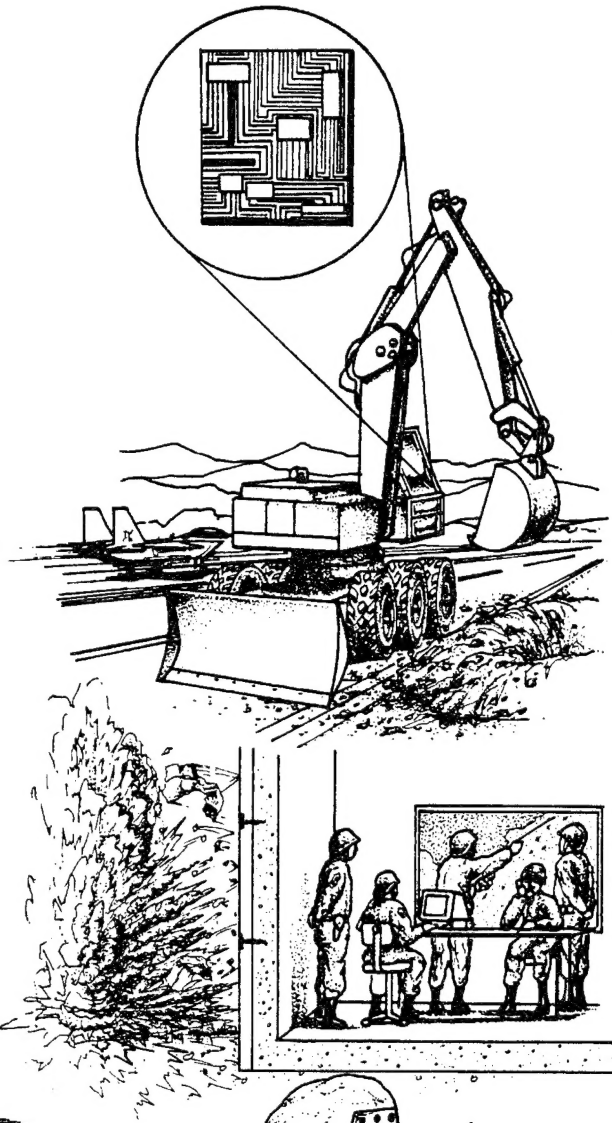

ESL-TR-92-07

MATERIALS FOR SHOCK MITIGATION

L. C. MUSZYNSKI, M. A. ROCHEFORT

APPLIED RESEARCH ASSOCIATES, INC.
POST OFFICE BOX 40128
TYNDALL AFB FL 32403-6001

JULY 1994

FINAL REPORT

OCTOBER 1989 - May 1991

APPROVED FOR PUBLIC RELEASE: DISTRIBUTION UNLIMITED

ENGINEERING RESEARCH DIVISION
Air Force Civil Engineering Support Agency
Civil Engineering Laboratory
Tyndall Air Force Base, Florida 32403

NOTICE

PLEASE DO NOT REQUEST COPIES OF THIS REPORT FROM HQ AFCESA/RA (AIR FORCE CIVIL ENGINEERING SUPPORT AGENCY). ADDITIONAL COPIES MAY BE PURCHASED FROM:

NATIONAL TECHNICAL INFORMATION SERVICE
5285 PORT ROYAL ROAD
SPRINGFIELD, VIRGINIA 22161

FEDERAL GOVERNMENT AGENCIES AND THEIR CONTRACTORS REGISTERED WITH DEFENSE TECHNICAL INFORMATION CENTER SHOULD DIRECT REQUESTS FOR COPIES OF THIS REPORT TO:

DEFENSE TECHNICAL INFORMATION CENTER
CAMERON STATION
ALEXANDRIA, VIRGINIA 22314

REPORT DOCUMENTATION PAGE

Form Approved
OMB No. 0704-0188

1. AGENCY USE ONLY (Leave Blank)	2. REPORT DATE	3. REPORT TYPE AND DATES COVERED
	July 1994	Final, 1 Oct 89-31 May 91

4. TITLE AND SUBTITLE
Materials for Shock Mitigation

5. FUNDING NUMBERS
C: F08635-88-C-0067

6. AUTHOR(S)
Muszynski, L.C. and Rochefort, M.A.

7. PERFORMING ORGANIZATION NAME(S) AND ADDRESS(ES)
Applied Research Associates, Inc.
P.O. Box 40128
Tyndall AFB, FL 32403

8. PERFORMING ORGANIZATION REPORT NUMBER

9. SPONSORING/MONITORING AGENCY NAME(S) AND ADDRESS(ES)
Air Force Civil Engineering Support Agency
Civil Engineering Laboratory
Engineering Research Division
Tyndall AFB, FL 32403-6001

10. SPONSORING/MONITORING AGENCY REPORT NUMBER
ESL-TR-92-07

11. SUPPLEMENTARY NOTES

12a. DISTRIBUTION/AVAILABILITY STATEMENT
Approved for public release.
Distribution unlimited.

12b. DISTRIBUTION CODE

13. ABSTRACT *(Maximum 200 words)*

The objective of this effort was to investigate basic material properties that affect shock wave attenuation in construction materials and field test materials which show promise as external shock mitigators (ESMs).

The results of this work demonstrated that very efficient ESM material systems can be produced from plastic containers embedded in low-density foam matrices. Full scale field testing was perfomed on such a material system using a conventional weapon.

14. SUBJECT TERMS
External Shock Mitigators
Backpacking Materials
Composite Materials
Ground Shock
Conventional Weapon Effects

15. NUMBER OF PAGES
74

16. PRICE CODE

17. SECURITY CLASSIFICATION OF REPORT	18. SECURITY CLASSIFICATION OF THIS PAGE	19. SECURITY CLASSIFICATION OF ABSTRACT	20. LIMITATION OF ABSTRACT
UNCLASSIFIED	UNCLASSIFIED	UNCLASSIFIED	UL

EXECUTIVE SUMMARY

A. OBJECTIVE

The objective of this research effort was to investigate basic material properties that affect shock wave attenuation in construction materials, and to field test materials which show promise as external shock mitigators (ESMs) for Air Force hardened facilities. The data developed provide an insight into shock-attenuation behavior of materials at high strain rates characteristic of high-intensity, short-duration loadings associated with close-proximity conventional weapon detonations.

B. BACKGROUND

The use of external shock-mitigating "backpack" materials surrounding a structure is one method of protecting a buried structure from the effects of blast loading. This method holds promise for retrofitting existing buried structures to provide additional protection from ground shock. By "backpacking" a buried structure, stress can be attenuated when a shock wave is transmitted through the backpacking material to the structure.

A suitable shock-absorbing backpacking material should be crushable and should possess a low compressive strength and a high degree of compressibility, thereby reducing the magnitude of peak stress reaching the structure, and accommodate the peak deformation of the backfill material without a sharp increase in stress above the compressive strength.

C. SCOPE

The scope of this effort included evaluating the efforts of other researchers in the field of ground shock structure-medium interaction, and testing novel construction materials which are potential ESMs. This effort included acquiring materials and equipment, sample preparation, testing, and analyzing response data. A field test was designed and conducted to evaluate two potential ESM systems.

D. EXPERIMENTAL CRITERIA

Materials that may mitigate the ground shock effects of close-in detonations of general purpose aerial munitions were evaluated. Assuming the detonation occurs at a sufficient scaled depth of burial for full energy coupling, that is, approximately 1.4 $ft/lb^{1/3}$ or greater; and at a scaled standoff of 2 $ft/lb^{1/3}$, the peak incident free-field stress may range from 200 to 10,000 psi, depending on the soil type and condition. For this type of scenario, the peak scaled free-field displacement may exceed 2 $in/lb^{1/3}$.(1)

E. RESULTS

The results of the field test verify the benefit of a new type of ESM material system, consisting of polyester terephthalate (PET) plastic bottles, embedded in a lightweight cellular foam grout. The resulting composite material is 77 percent air, by volume. Both this system and a conventional, "crushable" ESM material, bonded hollow, ceramic spheres, were field tested. A general-purpose, 1000-pound bomb was detonated 21 feet from the face of the NATO structure at the, Tyndall AFB Sky-10 test site, at a depth of burial (DOB) of 8.13 feet. One test panel, 3 feet square by 18 inches thick, was fabricated from each potential ESM material system. The bonded hollow ceramic sphere panel transmitted approximately 10 percent of the peak free-field ground shock stress, and was permanently crushed to about 50 percent of its original thickness. The grouted PET-ESM panel also transmitted only about 10 percent of the peak free-field ground shock stress, but the amount of permanent crushing was only 6 percent of its original thickness. The resulting crater was approximately 45 feet in diameter and 18 feet deep.

F. CONCLUSIONS AND RECOMMENDATIONS

1. Conclusions

The results of this work demonstrated that a very efficient external shock-mitigating (ESM) material system can be produced from plastic PET containers, embedded in a matrix of low-density foam. The field testing

demonstrated the utility of this ESM system, which transmitted only 10 percent of the peak free-field ground shock stress, and attenuated 96.1 percent of the ground shock impulse. Further work in the laboratory demonstrated that using a low-density, closed-cell, polyurethane foam as the binder instead of the cellular foam grout used in the field test, will enable the ESM material system to accommodate multiple ground shock events, whereas previous ESM material systems employed single-use, crushable material systems.

2. Recommendations

Perform further ground shock tests on optimized, low-density, closed-cell, polyurethane foam-PET bottle ESM designs, using multiple ground shock events, at the Tyndall AFB Sky-10 test facility.

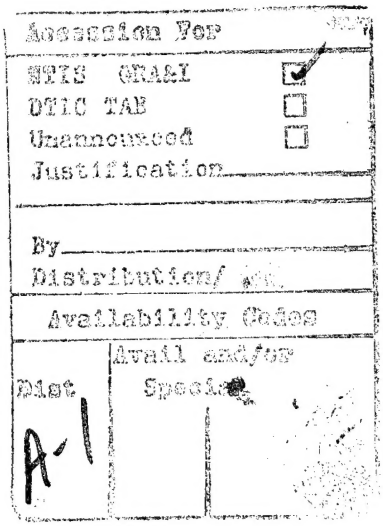

(The reverse of this page is blank.)

PREFACE

This report was prepared by Applied Research Associates, Inc. (ARA), P.O. Box 40128, Tyndall Air Force Base, Florida 32403, under contract F08635-88-C-0067, for the Air Force Civil Engineering Support Agency, Civil Engineering Laboratory, Engineering Research Division (AFCESA/RAC), Tyndall Air Force Base, Florida.

This report summarizes work done between 1 October 1989 and 31 May 1991. Captain Steve Kuennen and Walter Buchholtz were the AFCESA/RACS Project Officers for the subtask under which this work was accomplished.

This report has been reviewed by the Public Affairs Office and is releasable to the National Technical Information Service (NTIS).

This technical report has been reviewed and is approved for publication.

WALTER C. BUCHHOLTZ
Project Officer

WILLIAM S. STRICKLAND, GM-14
Chief, Airbase Survivability Branch

NEIL H. FRAVEL, Lt. Col, USAF
Chief, Engineering Research Division

FRANK P. GALLAGHER, Col, USAF
Director, Civil Engineering Laboratory

(The reverse of this page is blank.)

TABLE OF CONTENTS

TABLE OF CONTENTS
(CONTINUED)

LIST OF FIGURES

LIST OF FIGURES
(CONTINUED)

LIST OF FIGURES
(CONTINUED)

(The reverse of this page is blank.)

SECTION I

INTRODUCTION

A. OBJECTIVE

The objective of this research effort was to investigate basic material properties that affect shock wave attenuation in construction materials, and to field-test materials which show promise as external shock mitigators (ESMs) for Air Force hardened facilities. The data developed provide an insight into shock attenuation behavior of materials at high strain rates characteristic of high-intensity, short-duration loadings associated with close- proximity, conventional weapon detonations.

B. BACKGROUND

The structural design of buried protective structures to resist the effects of blast loading can be simplified if the structure can be designed to attenuate the stress wave when shock-loaded. Conservative designs of buried structures to resist blast loadings can result in costly solutions.

The use of external, shock-mitigating "backpack" materials surrounding a structure is one method of protecting a buried structure from the effects of blast loading. This method holds promise for retrofitting existing buried structures to provide additional protection from ground shock. By "backpacking" a buried structure, stress can be attenuated when a shock wave is transmitted through the backpacking material to the structure.

A suitable shock-absorbing backpacking material should be crushable and should possess a low compressive strength and a high degree of compressibility, thereby reducing the magnitude of peak stress reaching the structure, and should accommodate the peak deformation of the backfill material without a sharp increase in stress above the compressive strength.

The majority of compressible materials that fit these criteria fall into two categories: materials having no distinct yield point; and materials having a distinct yield point. These materials are referred to as plasto-elastic and elasto-plastic, respectively, as shown in Figures 1 and 2.

The amount of energy absorbed by the backpacking material can be determined by calculating the area under the stress-strain curves. Typically, elasto-plastic materials are more efficient energy absorbers than plasto-elastic materials, but they are also more costly.

C. SCOPE

The scope of this effort included evaluating the efforts of other researchers in the field of ground shock structure-medium interaction and testing novel construction materials which are potential ESMs. The effort also included acquiring materials and equipment, sample preparation, testing, and analyzing response data. A field test was designed and conducted to evaluate two potential ESM systems.

D. EXPERIMENTAL CRITERIA

Materials that may mitigate the ground shock effects of close-in detonations of general purpose aerial munitions were evaluated. Assuming the detonation occurs at a sufficient scaled depth of burial for full energy coupling, that is, approximately 1.4 $ft/lb^{1/3}$ or greater; and at a scaled standoff of 2 $ft/lb^{1/3}$, the peak incident free-field stress may range from 200 to 10,000 psi, depending on the soil type and condition. For this type of scenario, the peak scaled free-field displacement may exceed 2 $in/lb^{1/3}$.(1)

E. TECHNICAL APPROACH

1. Literature Review

A literature review was conducted to identify potential shock-mitigating materials that would reduce transmitted ground shock and

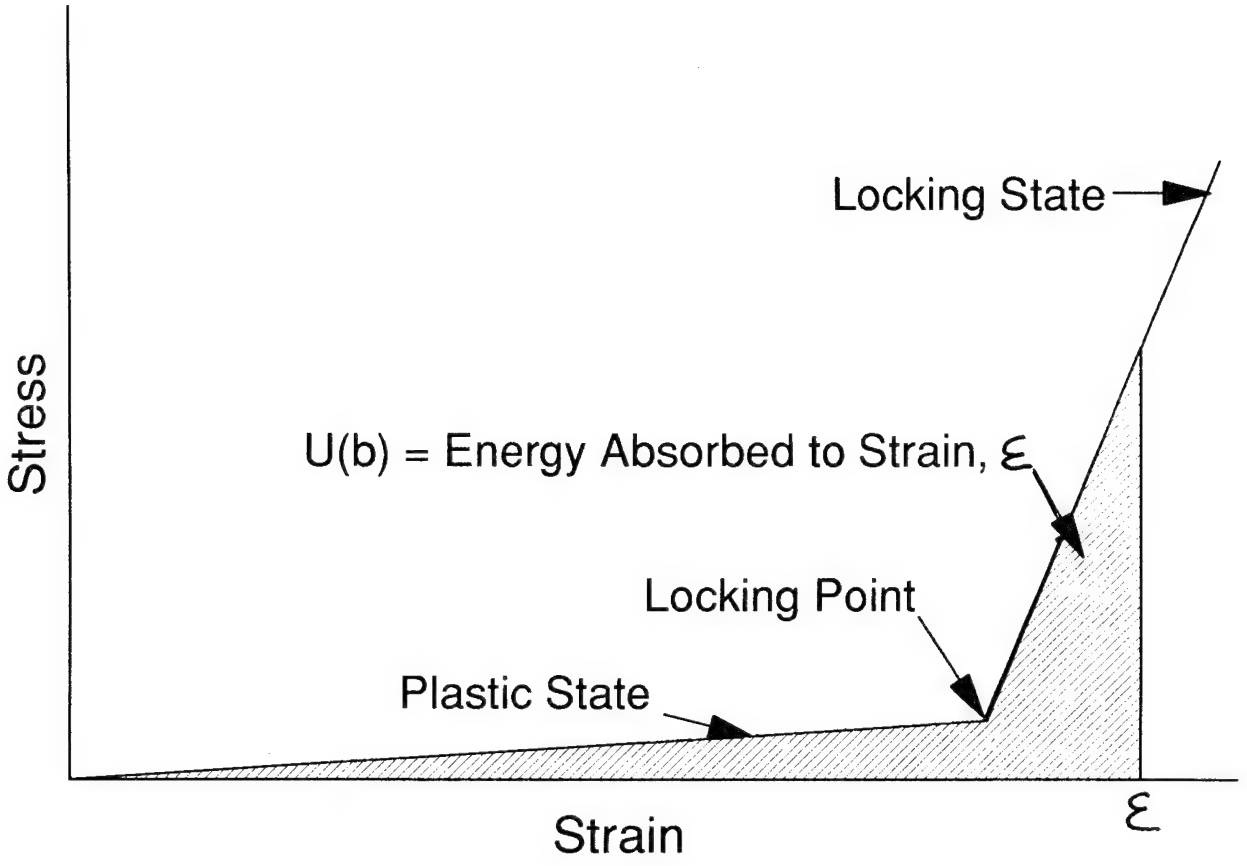

Figure 1. Stress-Strain Curve for Ideal Plasto-Elastic Material

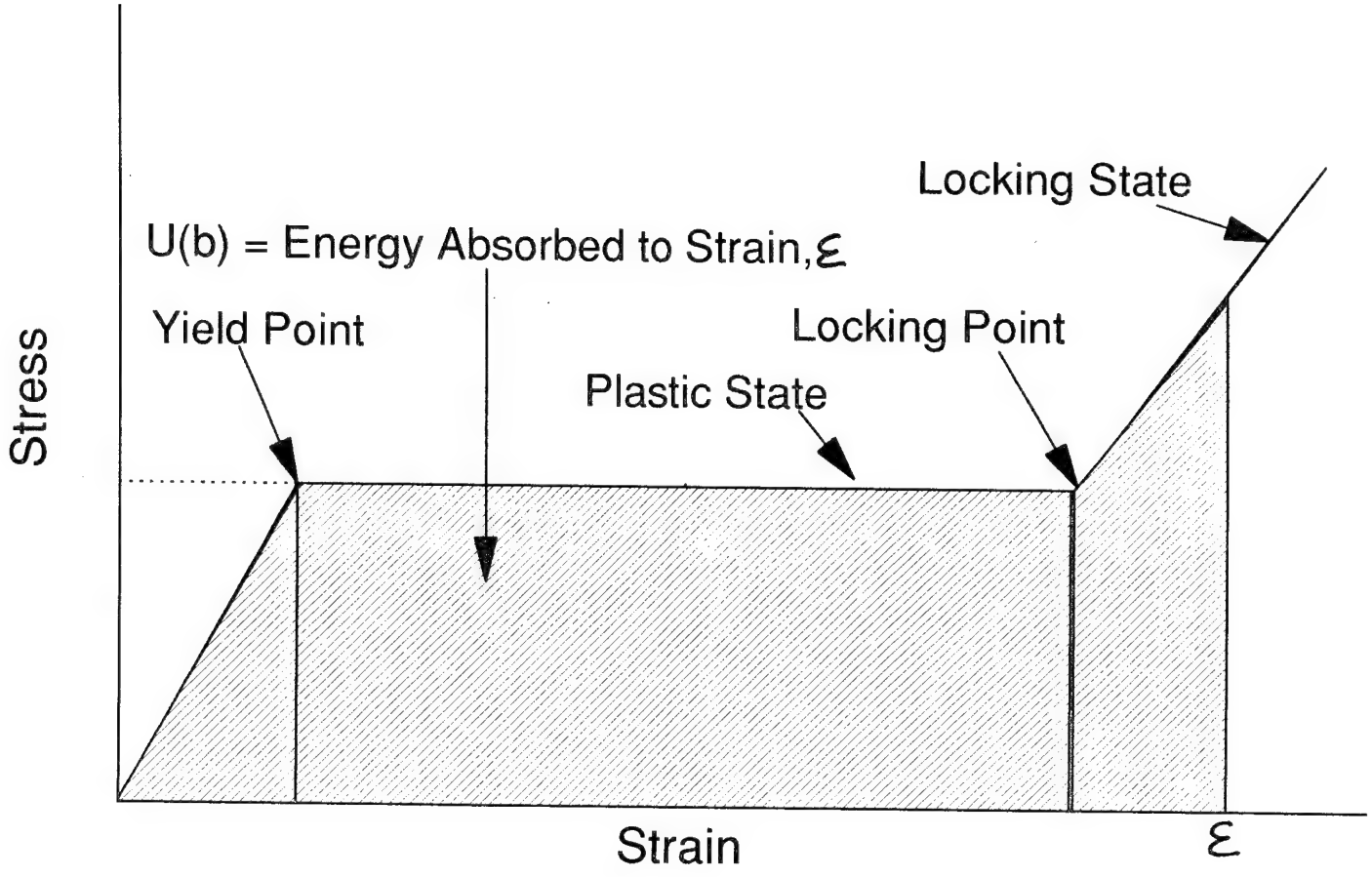

Figure 2. Stress-Strain Behavior for Ideal Elasto-Plastic Material

structural deformation. These materials may also be suitable for use in retrofitting buried Air Force structures. This literature review identified the efforts of others researching ground shock structure-medium interaction.

2. Selection Criteria

Criteria for selecting potential ESM materials were based on data obtained from other researchers, static and/or dynamic stress-strain curves of candidate materials, and economics. Final selection was based on field testing two candidate ESM material systems.

3. Laboratory Testing and Evaluation

Preliminary testing of candidate materials was performed in both static and dynamic modes. One candidate ESM material was tested using high strain rates in a Split-Hopkinson Pressure Bar (SHPB).

4. Field Testing and Evaluation

A full-scale field test was conducted at the Tyndall AFB Sky-10 test site. A general-purpose, 1000-pound bomb, buried at a DOB of 8.13 feet, was detonated 21 feet from the buried north basement wall of the NATO structure. Pressure gauges were attached to the buried concrete wall to record the incident and transmitted stresses.

SECTION II
LITERATURE REVIEW

The idea of using a "backpacking" material for shock isolation of buried structures is not new. In 1953, Engineering Research Associates, et al (2), in a report to the U.S. Army Corps of Engineers, dealing with the design of hardened tunnels in rock, suggested that "the space between the lining and the tunnel surface be filled with a material of low density that will absorb the energy of the flying rock, distribute the pressure from the fallen rock, and provide a mismatch of acoustic impedance so that reflection will take place at the tunnel surface rather than at the surface of the lining." In 1957, Vaile (3) reported on the beneficial use of frangible backfill (empty glass gin bottles) in isolating and protecting underground structures from violent ground motions in Operation PLUMBOB.

Sevin, et al (4,5) employed both flexible and rigid polyurethane foams and preexpanded polystyrene beads as crushable backfill to alleviate shock-induced motions of buried isolated structures. Da Deppo and Werner (6) also used crushable materials to reduce loads on buried structures.

Fowles and Curran (7) presented a theoretical description of the propagation of a pressure pulse in a potential backpacking material, and concluded that foamed or distended materials are effective in reducing the peak pressure delivered to a structure when an impulse is applied to the exterior surface of the backpack material. Smith and Thompson (8) concluded that placing a material having a low acoustic impedance between the structure and the confining medium will result in some of the shock energy being reflected and some absorbed.

Hoff (9) described two types of materials that exhibit ideal stress-strain behavior for use as backpacking. Plasto-elastic materials (Figure 1) are compressible, but do not possess a definite yield point; and elasto-plastic materials (Figure 2) are somewhat compressible, and do possess a definite yield point. Klotz (10) reported using plasto-elastic materials for shock-isolation purposes during the HARDHAT Shot of Operation NOUGAT.

Rempel (11) investigated rigid plastic foams and honeycombs, whose stress-strain relations approximate that of the ideal elastic-rigid locking solid, as an energy dissipating material. The advantage of these materials is that they can be preengineered to furnish almost any crushing stress level desired. The disadvantage of these materials is that they are much more expensive, relative to the plasto-elastic materials.

Hoff (21) describes cellular concretes, having unit weights of 20 to 50 lbs/ft^3 and air contents as high as 75 percent by volume, as "elasto-plastic materials" that provide the desired shock-isolation characteristics required of a backpacking material. He also discusses design criteria for a backpacking system (13), and concludes that it should be of sufficient thickness to accept twice the expected deformation of the backfill material, assuming single-burst loading.

Hinckley and Yang (14) analyzed rigid-plastic polyurethane foams having various unit weights, as impact shock mitigators at varying strain rates. They concluded that the strain rate effect decreases as the unit weight of the foam decreases, and that polyurethane foam is a very effective shock-mitigating material, as long as it does not experience lockup. Lockup refers to closure of the foam pores to the extent that the foam behaves as a solid material. Stresses greater than the yield stress cannot be transmitted by such materials until lockup occurs. The point on the curve where this second elastic or "pseudo-elastic" region begins is called the lockup point, and is usually defined by a percent strain. Hinckley and Yang also developed a computer program that adequately predicts the force transmitted by the mitigator as a function of time, and the energy absorbed by the mitigator.

Denson, Ledbetter and Saylak (15) investigated 28 possible backpacking material systems, of which six were chosen as viable candidates. The six material systems were: expanded polystyrene concrete, expanded polystyrene concrete with fly ash, cellular concrete with fly ash, foamed sulfur concrete, rigid polyurethane foam, and molded expanded polystyrene. The candidate materials were subjected to confined static and dynamic compressive stress. Lockup usually occurred at about 40 percent strain. Tensile strain capacity,

creep, density, water absorption, specific heat, coefficient of thermal expansion, thermal conductivity, and flammability were all determined for the six viable candidate material systems in this study.

SECTION III
SELECTION CRITERIA

A. EXTERNAL SHOCK MITIGATOR (ESM) PRINCIPLE

The basic requirement for external shock-mitigating (ESM) materials is that they possess certain characteristics associated with dynamic structure-medium interaction. The ESM material should dissipate incoming ground shock energy, reduce the input stress reaching the structure, and accommodate the deformation of the backfill surrounding the structure. Dynamic structure-medium interaction, due to ground shock resulting from detonating a conventional weapon below the ground surface, can be illustrated by three springs in series, the first representing the backfill, the second representing the ESM material, and the third representing the wall of a buried structure. Simply stated, the resistance of the ESM needs to be less than that of the wall, to accommodate the displacement of the backfill and reduce the deflection of the wall.

B. MATERIALS

Materials that appear to perform satisfactorily as external shock mitigators are referred to as plasto-elastic and elasto-plastic.

Examples of elasto-plastic materials include:

- Rigid Polyurethane foam
- Rigid Polystyrene foam
- Syntactic foam
- Cellular concrete
- Inorganic foam

Examples of plasto-elastic materials include:

- Expanded clay, shale, and slag
- Perlite & Vermiculite
- Flexible Organic foam
- Foamed Rubber
- Organic and Inorganic microballoons
- Expanded Polystrene beads

Elasto-plastic and plasto-elastic materials can be further divided into two other classes of materials based on their chemical composition, that is, organic and inorganic materials.

1. Organic Materials

Organic foam, such as polyurethane foam, exhibits elastic, nearly perfectly-plastic stress-strain behavior until lockup occurs at large strain. Stress greater than yield cannot be transmitted until lockup occurs starting at the plateau stress shown in Figure 3.

Figures 4, 5, and 6 illustrate the static and dynamic stress-strain behavior of polyurethane foam having unit weights of 3.5 lbs/ft^3, 7.0 lbs/ft^3, and 14.5 lbs/ft^3 respectively (14). Figure 7 illustrates the strain rate dependence of the compressive yield stress of polyurethane foam at the above-mentioned unit weights (14). Apparently, both the degree of strain rate dependence, and the compressive yield stress itself decrease as the density of polyurethane foam decreases. This becomes important when designing an ESM material, to allow only a certain magnitude of stress to be transferred to the structure at a given strain rate prior to lockup.

2. Inorganic Materials

Cellular concretes, polymer modified concretes and foamed, inorganic binders have also been shown to operate satisfactorily as ESM materials, based on their stress-strain behavior. Figures 8, 9, and 10 illustrate the stress-strain behavior of 45 lbs/ft^3 fly ash-modified cellular concrete, expanded polystyrene bead concrete at 45 lbs/ft^3, and foamed sulfur concrete at 36.5 lbs/ft^3 respectively. These tests were performed by Denson et al., (15) under a confined condition, loaded in static compression. Figure 11 illustrates the effect of density on the stress-strain behavior of foamed sulfur concrete. From these data, it appears that ESM materials become more efficient as their density decreases, that is, they exhibit "more perfect" plastic behavior.

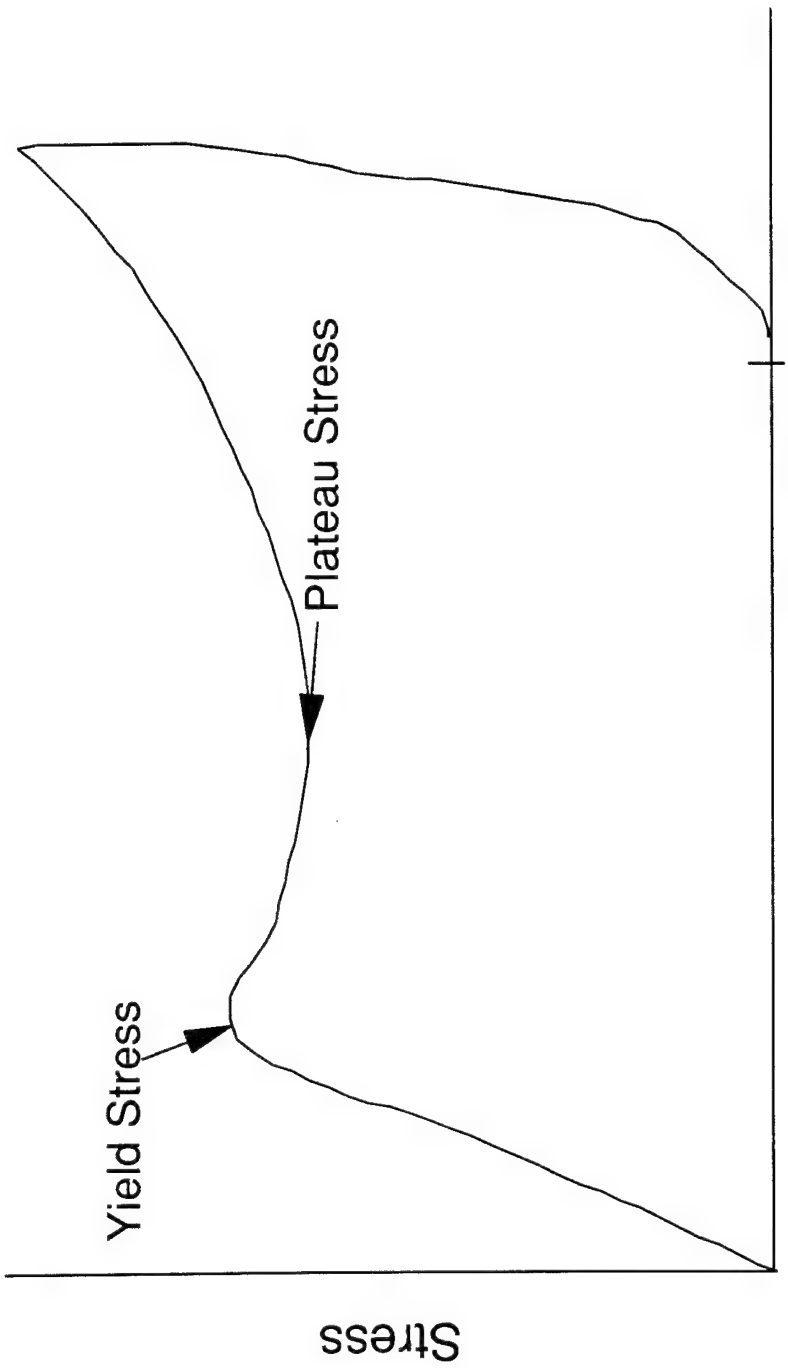

Figure 3. Typical Stress-Strain Curve for Rigid Polyurethane Foam (14).

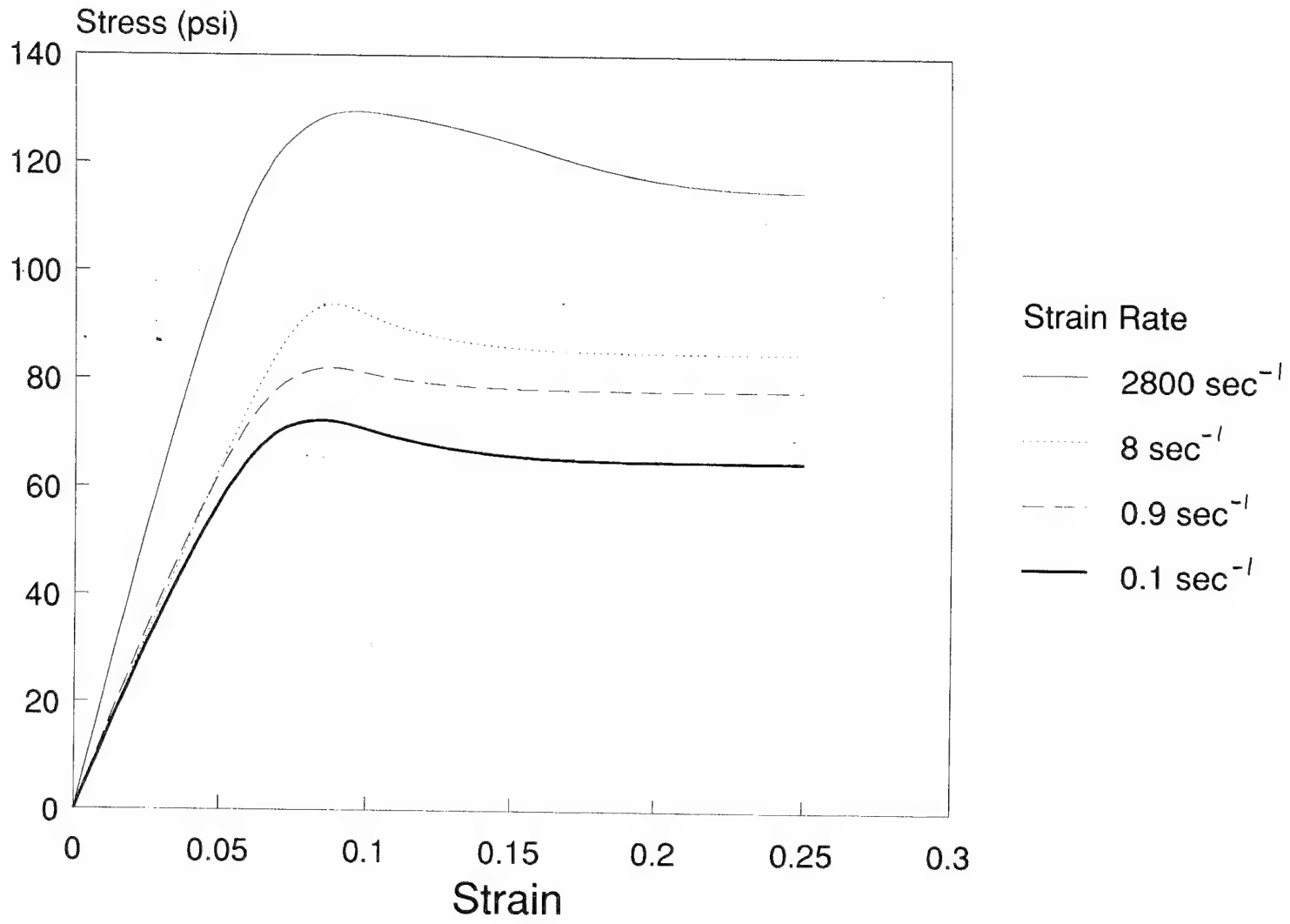

Figure 4. Typical Stress-Strain Curves for 3.5 lbs/ft^3 Rigid Polyurethane Foam (14)

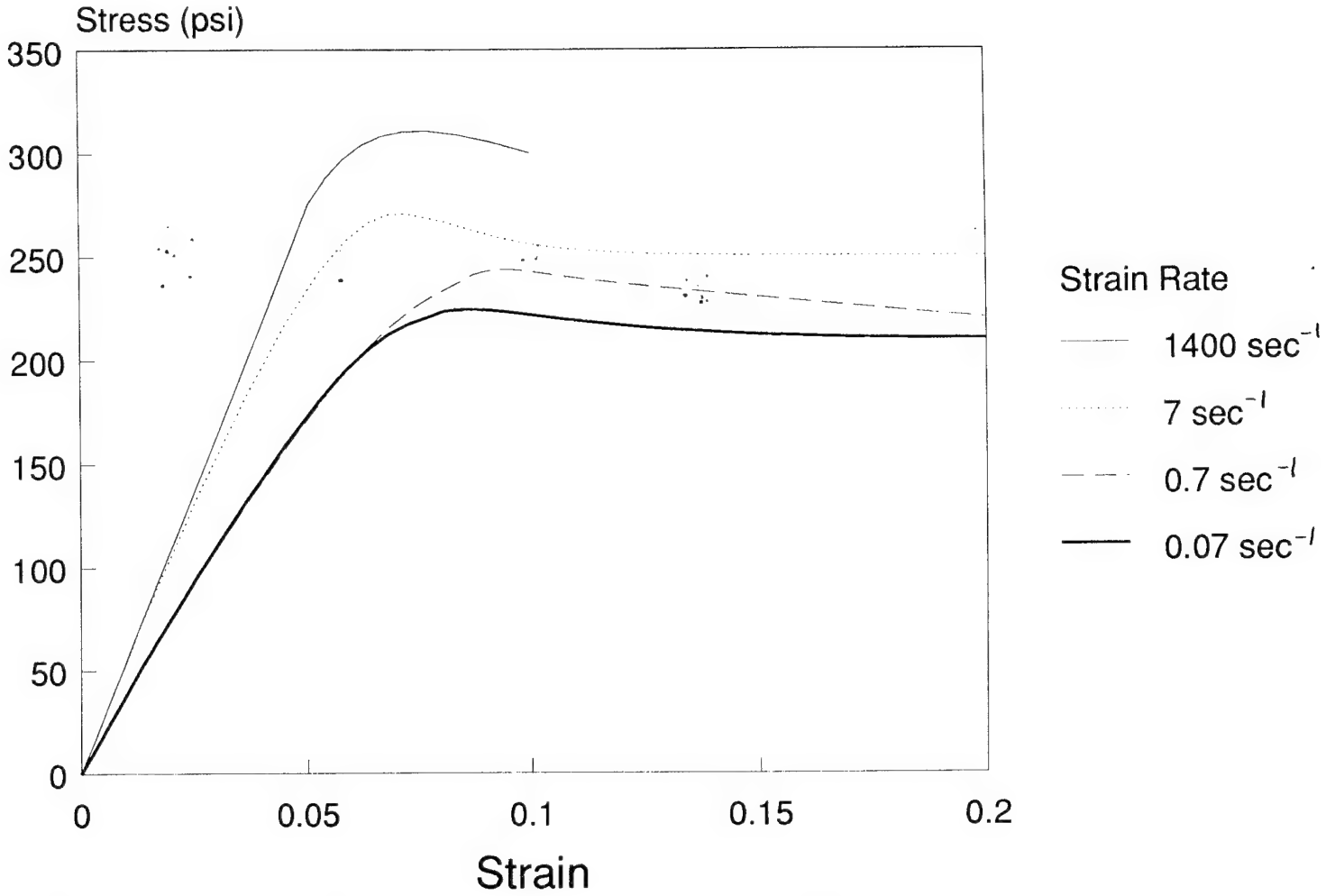

Figure 5. Typical Stress-Strain Curves for 7.0 lbs/ft^3 Rigid Polyurethane Foam (14)

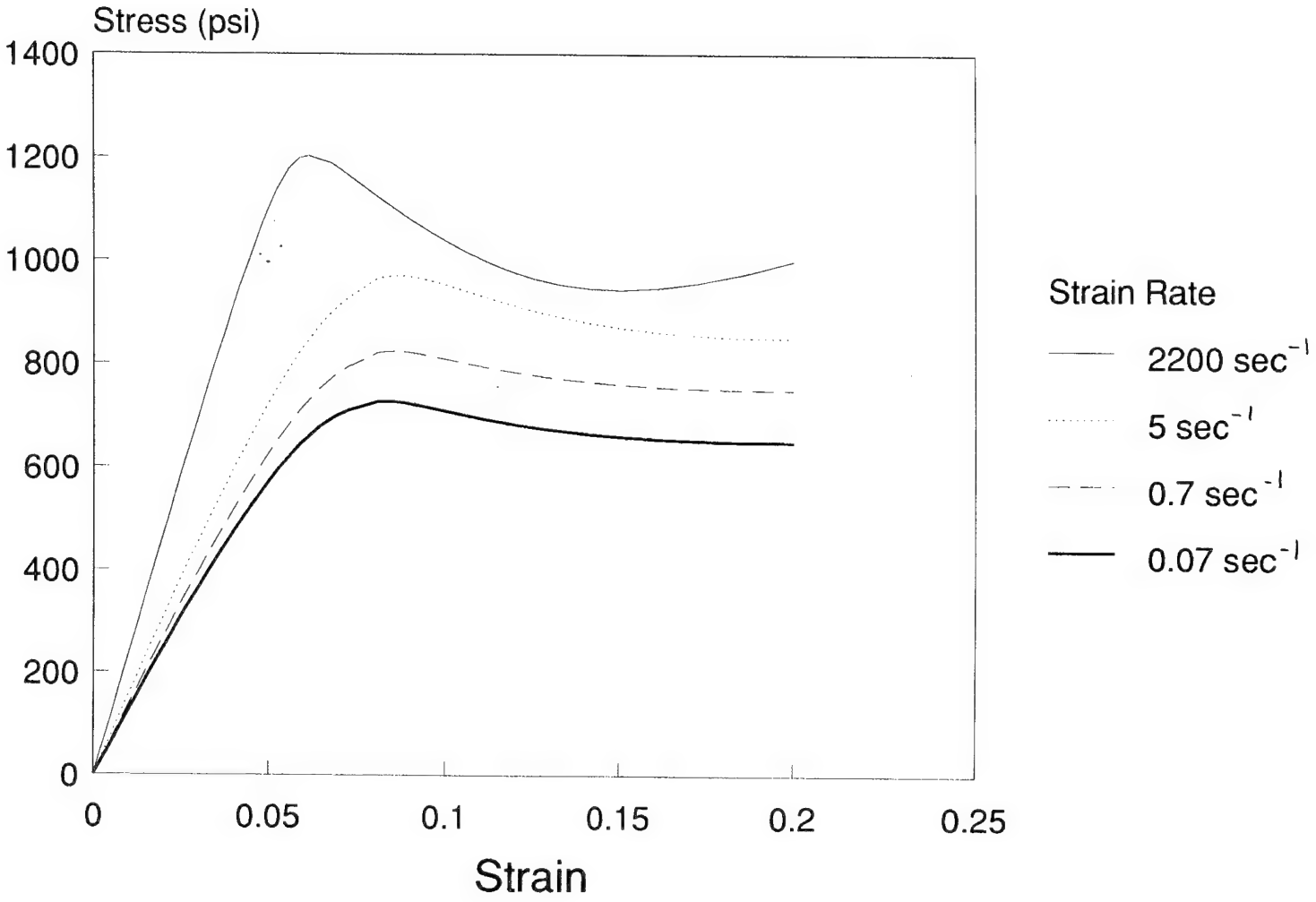

Figure 6. Typical Stress-Strain Curves for 14.5 lbs/ft^3 Rigid Polyurethane Foam (14)

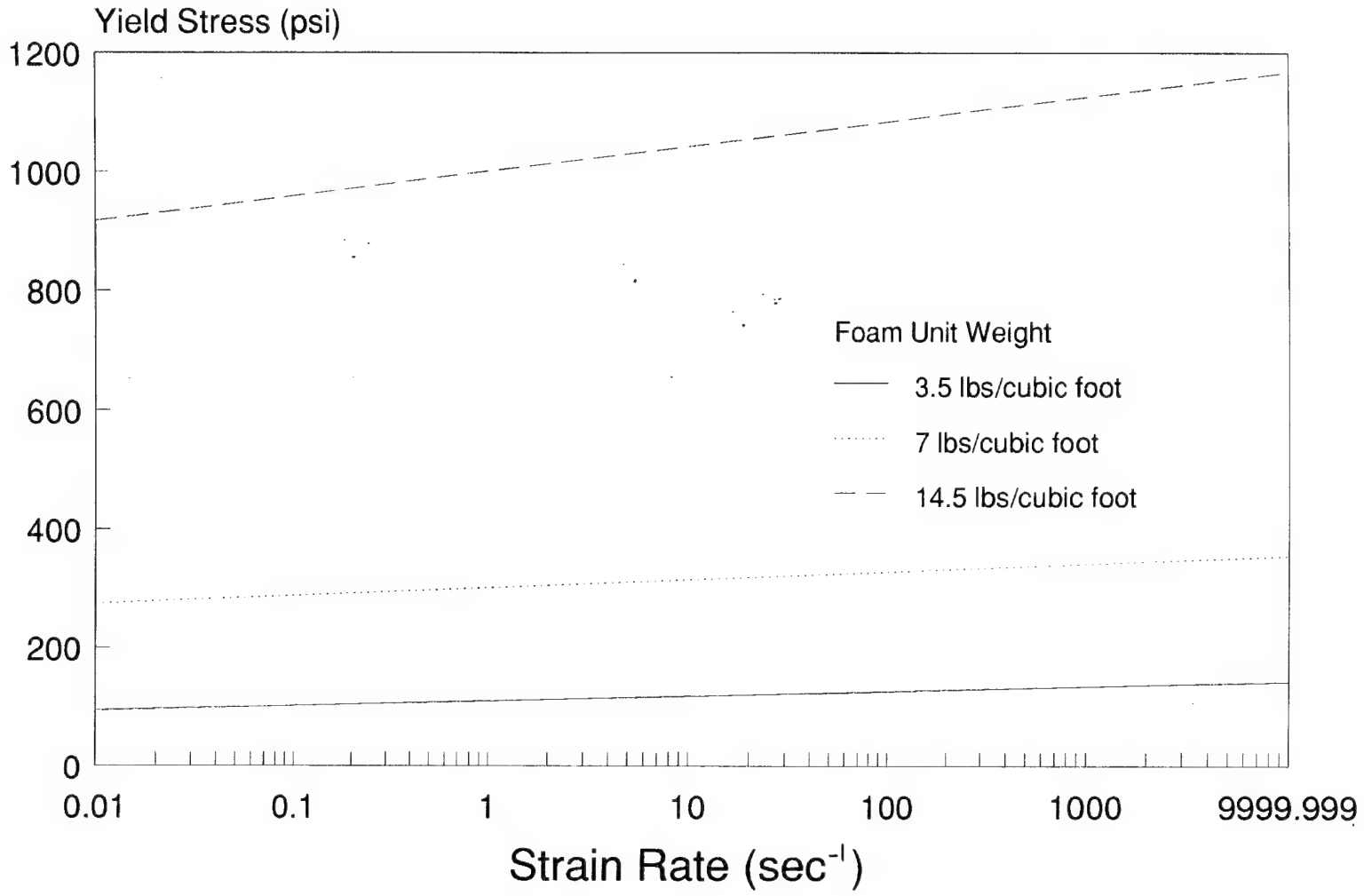

Figure 7. String Rate Dependence of Compressive Yield Strength of Rigid Polyurethane Foam (14)

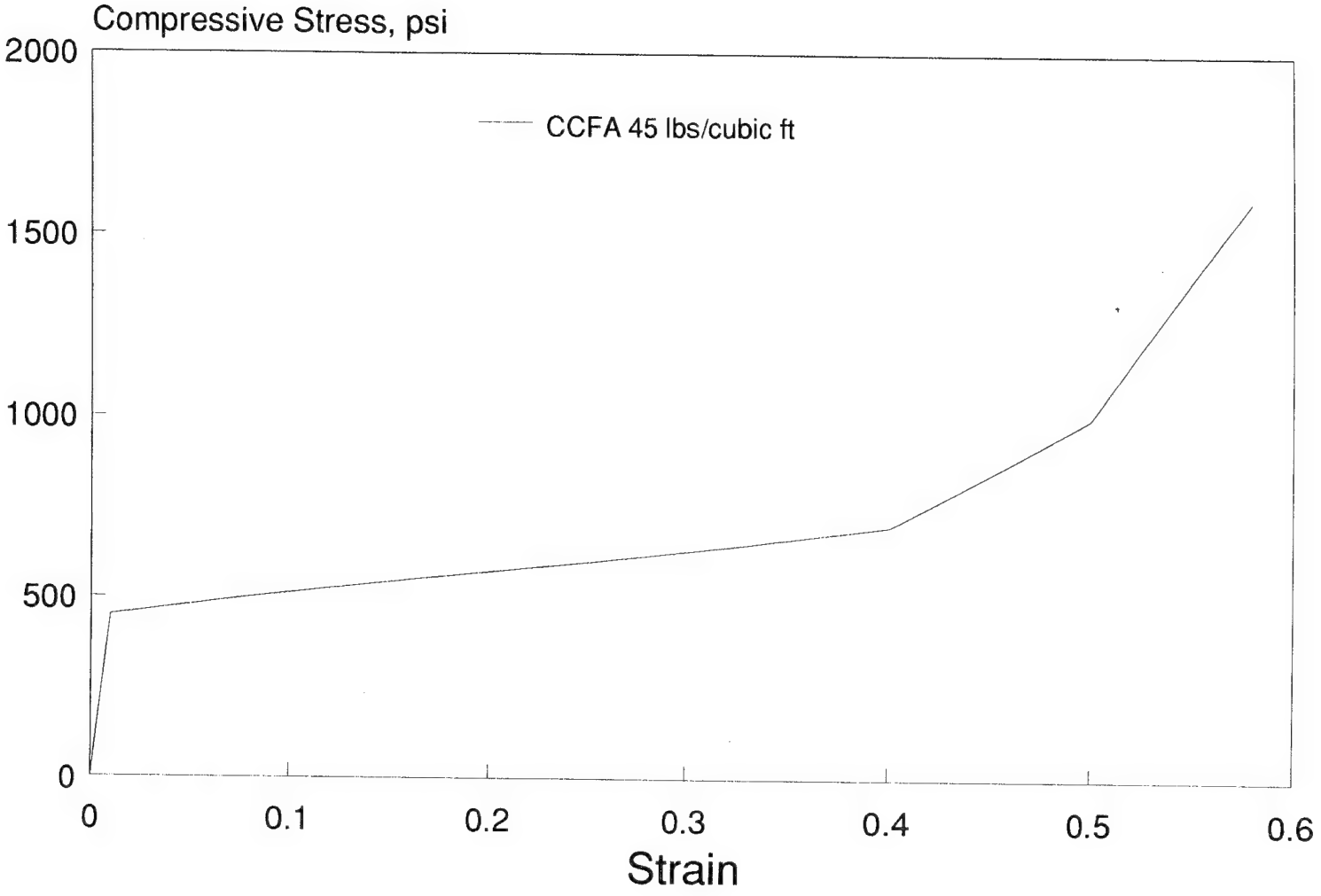

Figure 8. Confined Static Compressive Test Result for CCFA 45 (15).

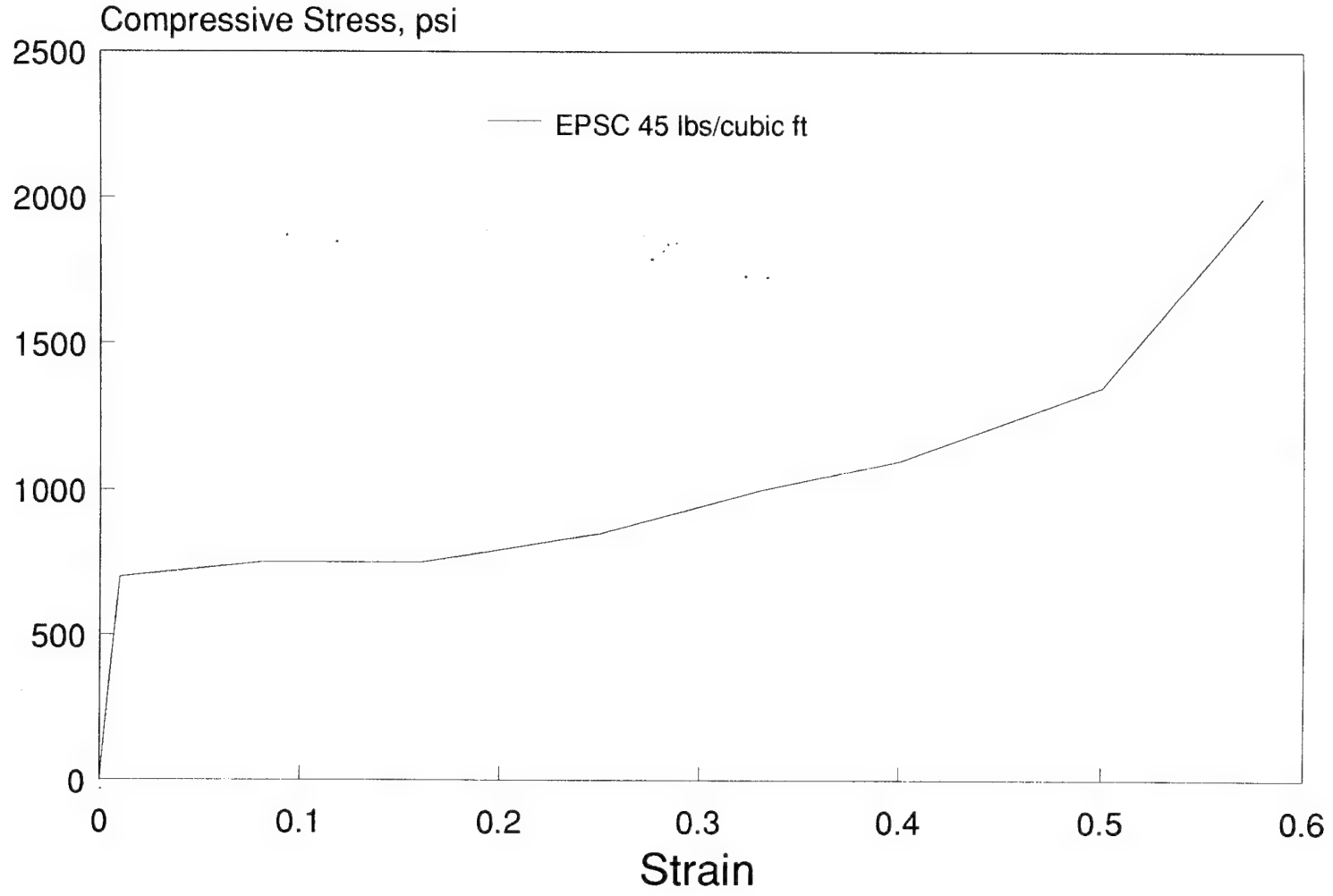

Figure 9. Confined Static Compressive Test Results for ESPC 45 (15)

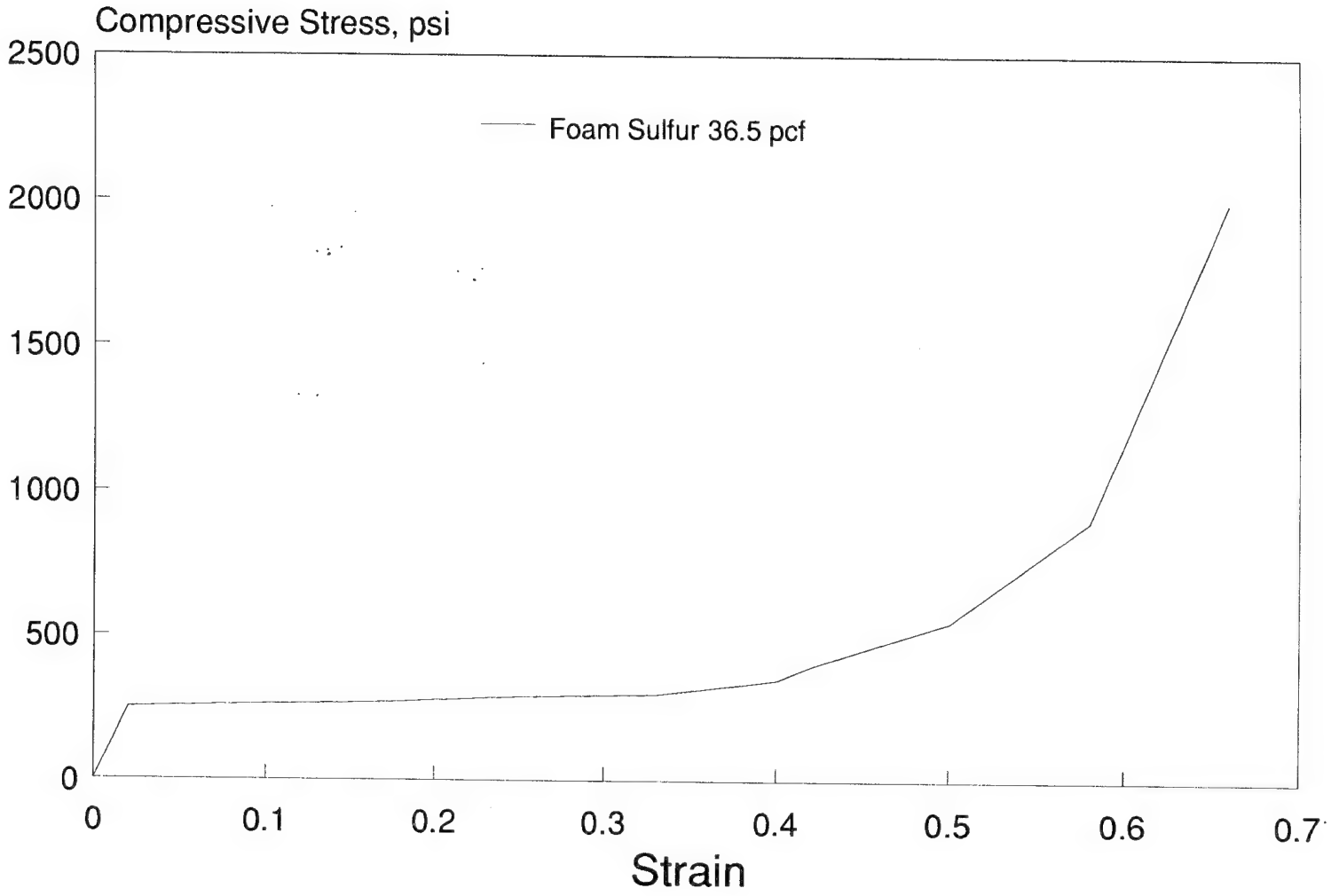

Figure 10. Confined Static Compressive Result for FS 36.5 (15)

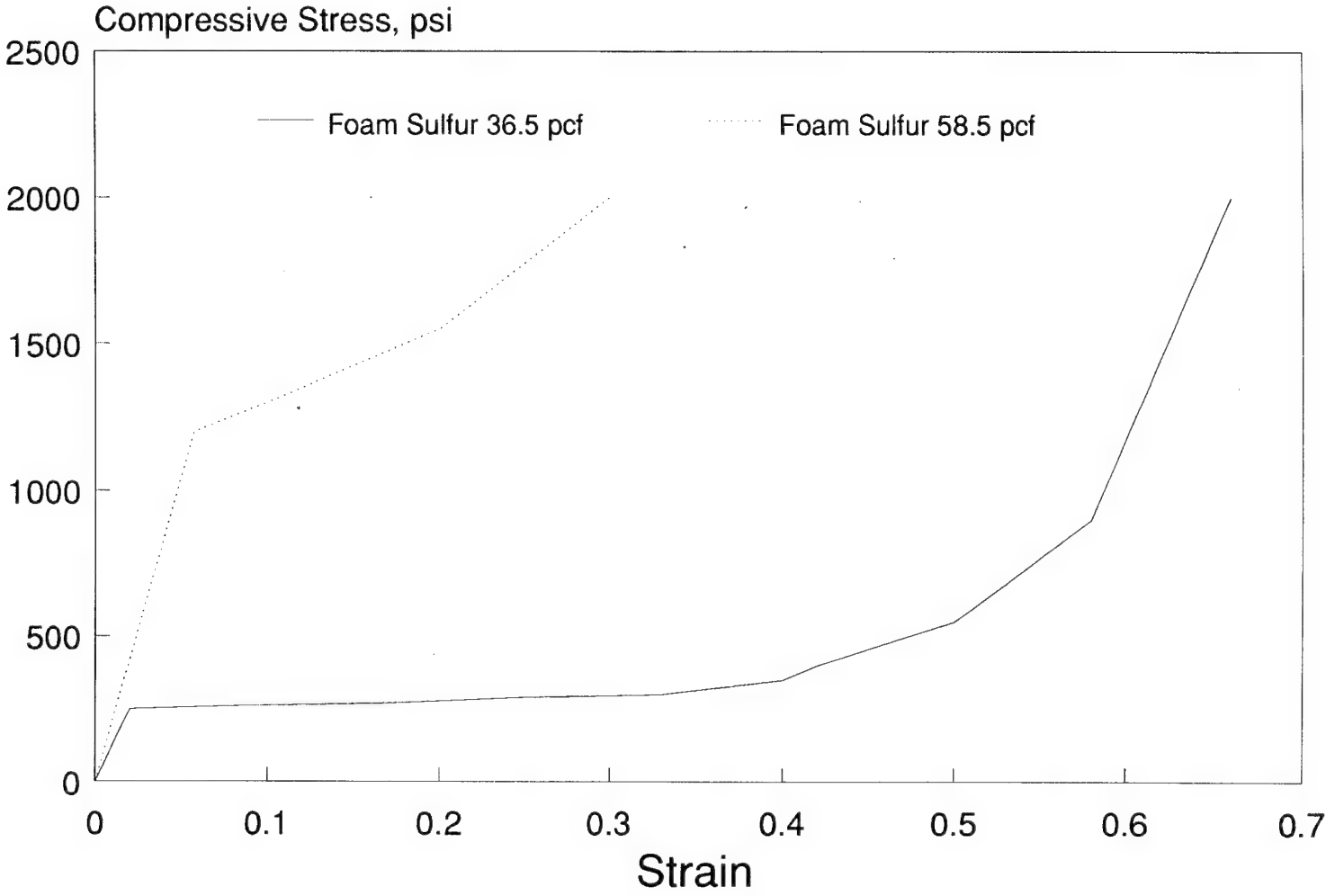

Figure 11. Confined Static Compressive Result for FS 36.5 and FS 58.5 (15)

C. CONCLUSIONS

Based on the results of Hinkley and Yang (14) and Denson, et al.(15), the performance requirements of an effective ESM material are as follows:

1. Confined yield stress of approximately 100 to 1000 psi.
2. Static compressive stress-strain behavior similar to that of an ideal elasto-plastic material,
3. Lockup at approximately 40 percent strain,
4. Closed-cell structure,
5. Capable of being precast or cast in place using conventional construction equipment.

SECTION IV
LAB EVALUATION OF CANDIDATE ESM MATERIALS

A. INTRODUCTION

The literature survey proved extremely valuable in the evaluation of potential candidate ESM materials. This work has been ongoing since the 1950s. It was decided that the testing and evaluation process would entail both traditional test methods, such as confined and unconfined compressive stress-strain curves, and unconventional methods such as the Split Hopkinson Pressure Bar (SHPB).

Two candidate materials were thoroughly investigated. Hollow ceramic spheres, which are manufactured and distributed by 3M Corporation under the tradename Macrolite® Ceramic Spheres, were utilized as a syntactic inorganic foam. These hollow, ceramic spheres are made by a proprietary process that enables them to be very durable and lightweight.

A new and unique system was also proposed and tested. This system makes use of a novel method of incorporating large volumes of confined and entrapped air in a cementitious matrix. Empty polyester terephthalate (PET) bottles sealed with the caps in place were packed into a mold and infiltrated with a cellular cementitious material using a process similar to that used with preplaced aggregate concrete. The matrix was prepared using portland cement, water, and a chemical surfactant, to produce a lightweight cellular matrix having a dry unit weight of approximately 67 lbs/ft^3.

B. STATIC STRESS-STRAIN TESTING

1. Bonded Hollow Ceramic Spheres

The Macrolite® (ML 535) hollow ceramic spheres used in this part of the laboratory effort had a size range of 5.7mm to 12.7mm, and a unit weight of 19 lbs/ft^3. The spheres were bonded using an ordinary epoxy resin, at a concentration of 2 parts per hundred resin (phr), and having a viscosity of 500

centipoise at 25°C. The syntactic foam composite was ambient cured for 24 hours.

Figures 12 and 13 show static unconfined and confined compressive stress-strain curves for the bonded hollow ceramic spheres. In the unconfined state, the material was crushed, failing at a very small strain and producing a stress-strain curve similar to that of an ideal plasto-elastic material. In the confined (uniaxial strain) condition, the material behaved like an ideal elasto-plastic material, and experienced lockup at about 20 percent strain.

2. Cellular Grouted PET System

The cellular grout binder for the PET ESM material system was also tested, and the unconfined static compressive stress-strain curve is shown in Figure 14. The material appears to behave like an ideal plasto-elastic material. The static confined compressive stress-strain curve could not be generated in the lab because of load cell capacity restrictions.

C. SPLIT-HOPKINSON PRESSURE BAR

Figure 15 shows the Split-Hopkinson Pressure Bar (SHPB) apparatus used to determine the dynamic, confined, compressive stress-strain behavior of the hollow ceramic spheres. Figure 16 shows the plexiglass confinement chamber, fabricated to photograph the event, using high- speed photography. The principle of the SHPB, illustrated schematically in Figure 17, is simple. A gas pressure-driven striker bar impacts the incident bar (bar no. 1), which induces a compressive stress pulse in the incident bar. The sample is sandwiched between the incident bar and the transmitter bar (bar number 2). When the incident compressive pulse reaches the sample, part of the incident pulse is reflected, and part is transmitted through the sample to bar number 2. The transmitted strain pulse and the integral of the reflected strain pulse are proportional to the stress and strain in the specimen, respectively (Reference 16).

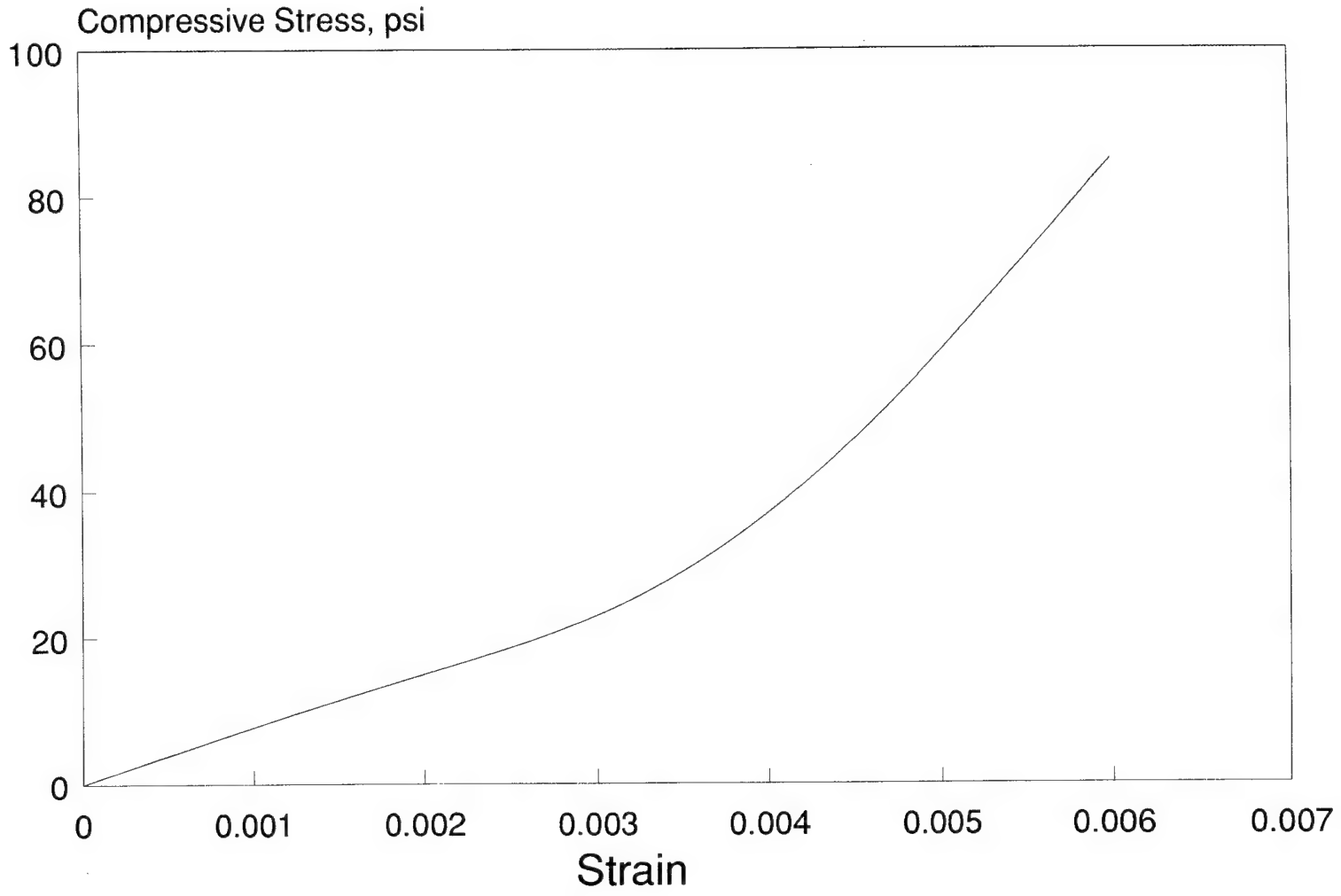

Figure 12. Unconfined Static Compressive Stress-Stain Curve of Bonded Hollow Ceramic Spheres

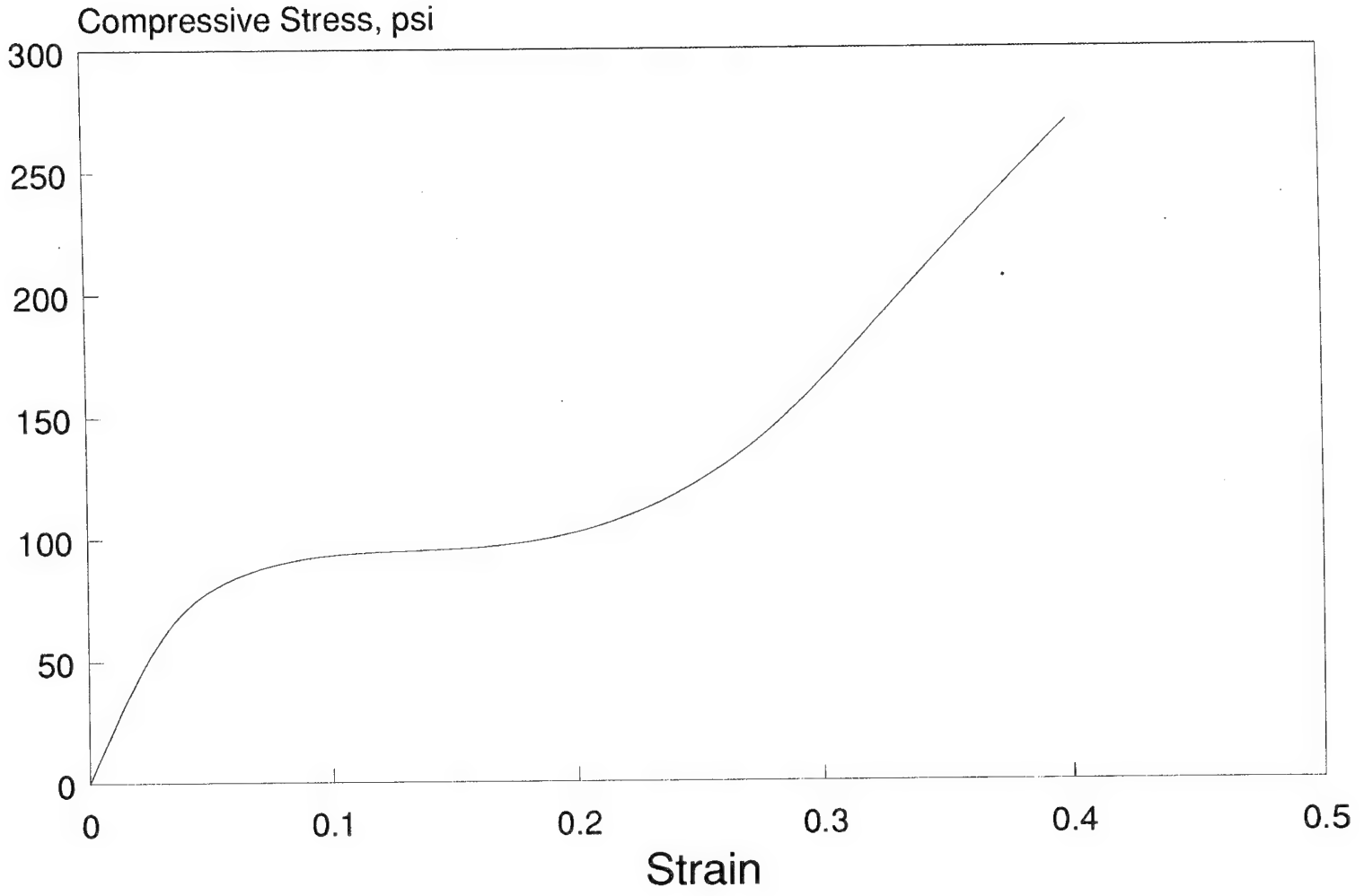

Figure 13. Confined Static Compressive Stress-Strain Curve of Bonded Hollow Ceramic Spheres

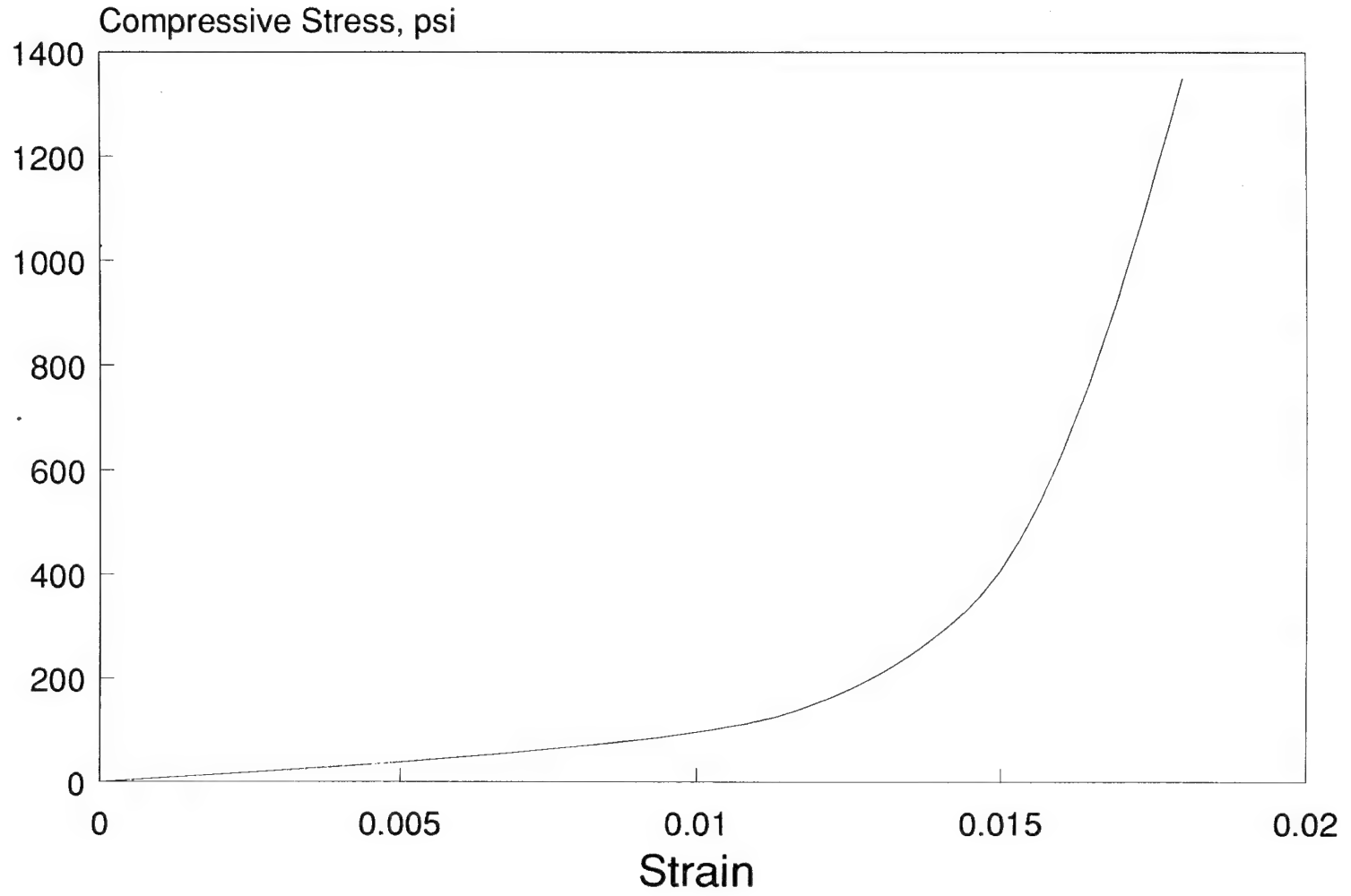

Figure 14. Unconfined Static Compressive Stress-Strain Curve of the PET-ESM System Cellular Grout Binder.

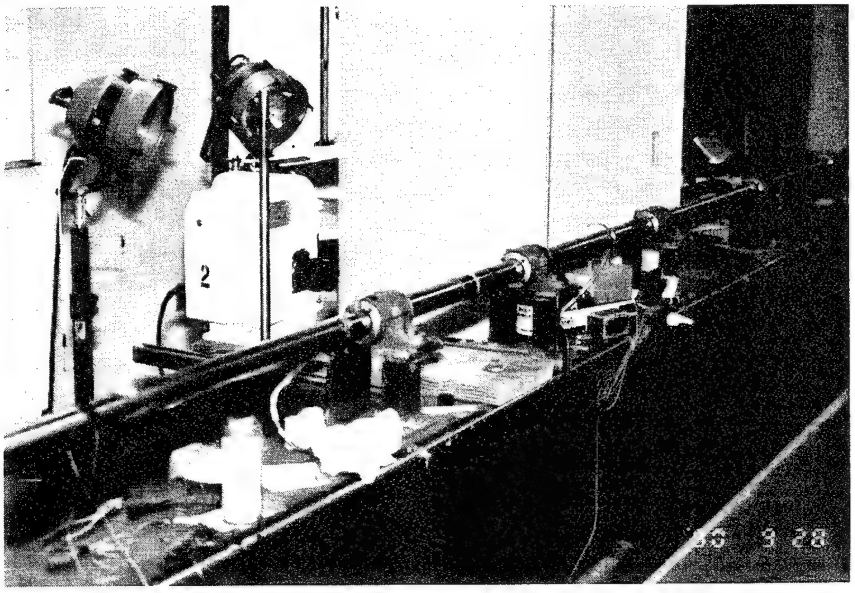

Figure 15. RACS Split Hopkinson Pressure Bar (SHPB) Apparatus.

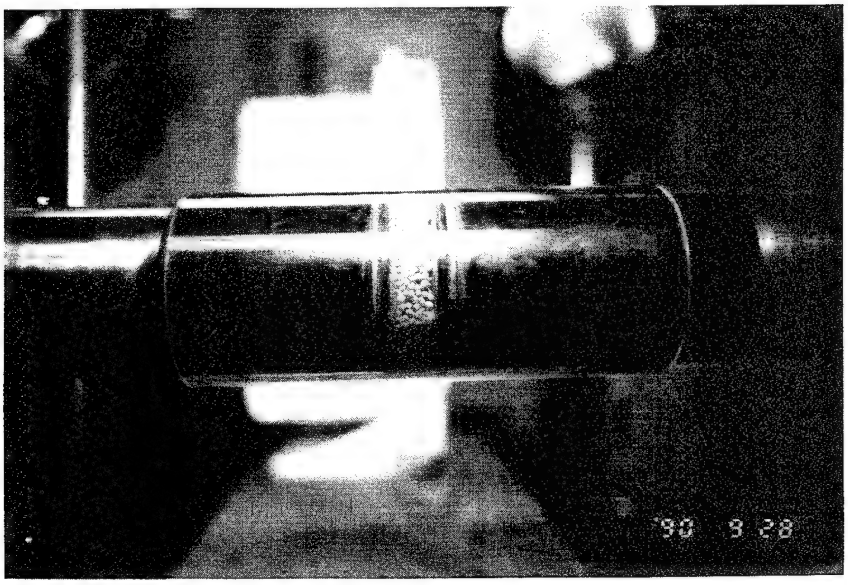

Figure 16. Confined Dynamic Compressive Strength Specimen in RACS SHPB Apparatus (BHCS)

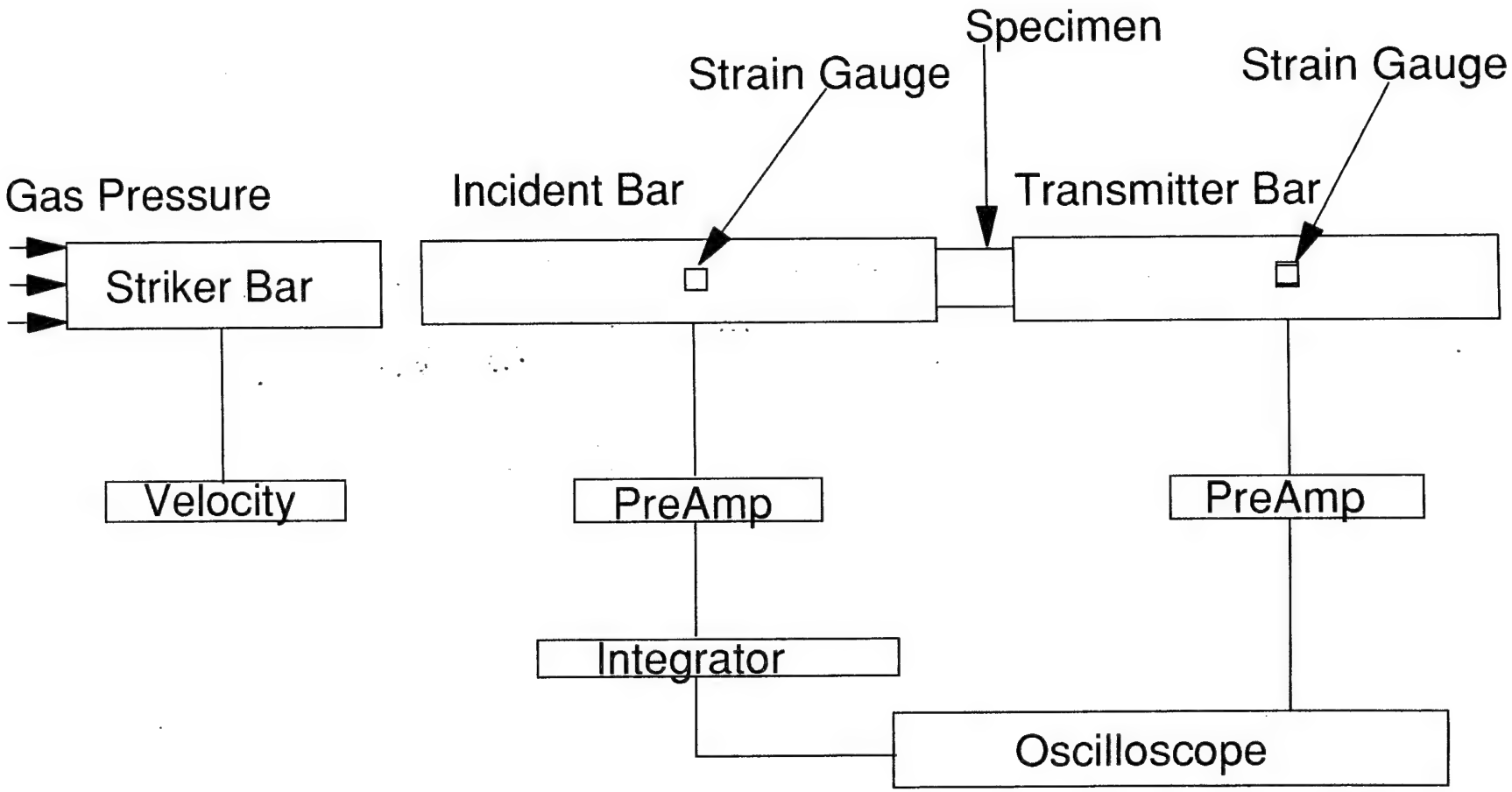

Figure 17. Split Hopkinson Pressure Bar Schematic

Figure 18 shows a dynamic, confined stress-strain curve for an SHPB test on the Macrolite® hollow ceramic spheres. Sample 714 had sphere diameters ranging between 1.4mm and 2.8mm, and a unit weight of 25 lbs/ft^3. The small sphere diameters were necessary because the RACS SHPB is limited to a maximum sample diameter of 5 cm. The magnitude of the incident compressive stress pulse is determined by the gas gun pressure applied to the striker bar, which for these tests was 50 psi and caused a 27 ksi compressive stress pulse in the incident bar.

The cellular grout binder was not tested in the SHPB apparatus. Its friable nature made it impossible to obtain any meaningful data at high strain rates, because the sample disintegrated.

D. CONCLUSIONS

Ideal ESM material systems will accommodate large free- field displacements, while transmitting small loads to the shelter. To adequately test ESM materials, specimens must be subjected to large strains (up to approximately 50 percent). The current RACS SHPB setup is not capable of straining specimens to this level. The loading pulse is too short (striker bar too short). Also, the ESM material samples could not be made small enough for SHPB testing. The SHPB is better suited for testing small, homogeneous materials, such as metals, cement paste, and mortar. Therefore, the stress-strain relationships of the ESM systems tested in the field, which control their ability to attenuate ground shock associated with a close-proximity, conventional weapon detonation, are best determined by a confined static compression test on a sample large enough to be representative of the in situ material.

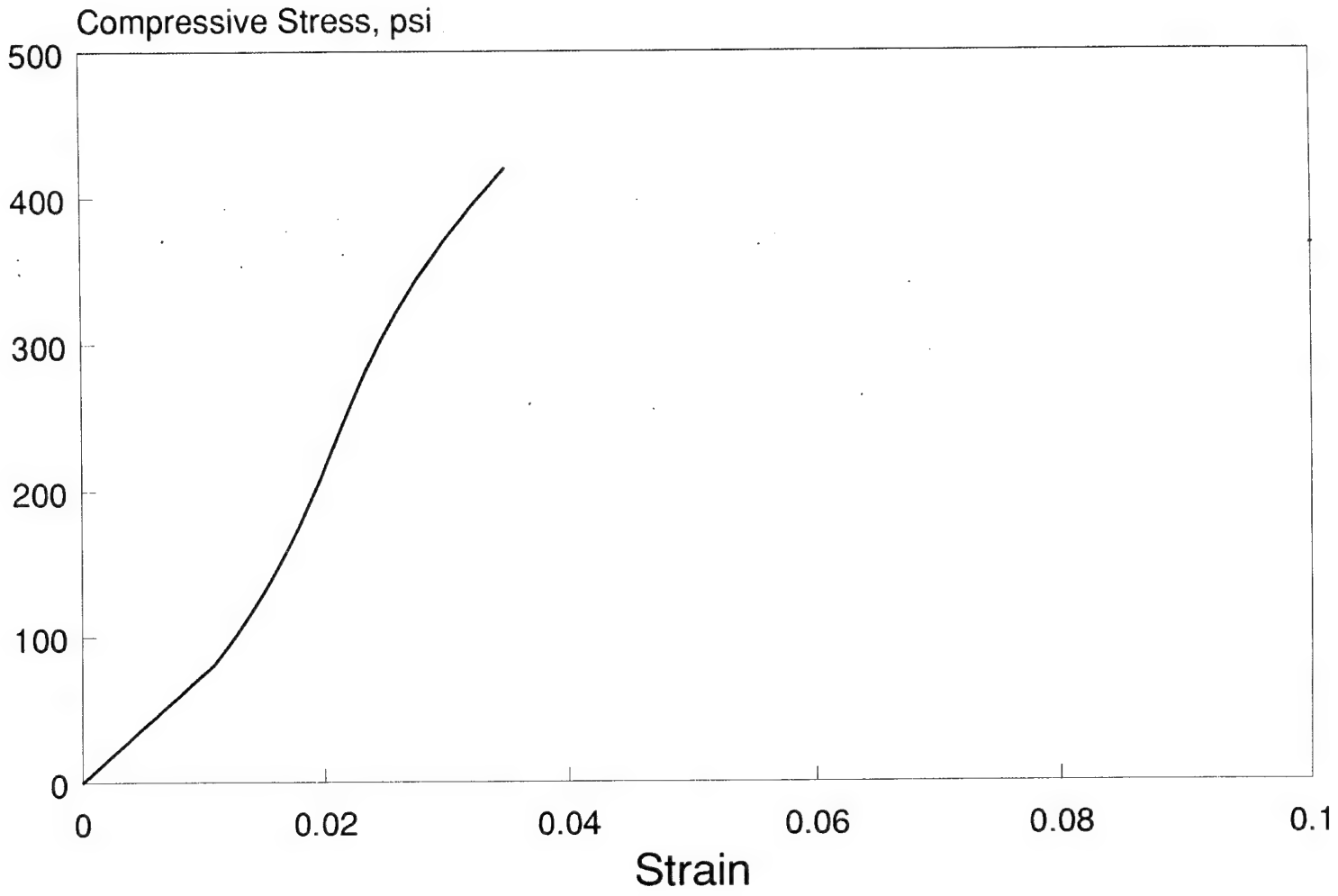

Figure 18. Confined Dynamic Compressive Stress-Stain Curve of Bonded Hollow Hollow Ceramic Spheres Using SHPB

SECTION V
FIELD DEMONSTRATION

A. BACKGROUND

A full-scale field demonstration was performed, incorporating a 1000 pound, general-purpose bomb, detonated against a buried basement wall of the NATO structure at the Tyndall AFB Sky-10 test site. The demonstration was performed to evaluate a current, state-of-the-art syntactic foam ESM material system, as well as an entirely new system, consisting of grouted PET bottles.

B. TEST PLAN

Figure 19 illustrates the test site layout proposed for the two candidate ESM materials. Figure 20 shows the expected crater profile, from the denotation located on the north side of the NATO structure.

1. Test Description

The ESM systems were mounted against the basement wall of the NATO structure, equidistant from the center of gravity of the 1000-pound bomb, which was located 8.13 feet below the ground surface. Four pressure gauges were also placed equidistant from the bomb center of gravity. Gauges SI-2 and SI-3 were embedded in the bare concrete basement wall. Gauge SI-1 was centered and located directly behind the ESM material consisting of bonded hollow ceramic spheres (BHCS). Gauge SI-4 was centered and located directly behind the ESM material consisting of grouted PET (GPET) bottles. The standoff distance for the bomb was 21 feet from the NATO structure (19.5 feet from the ESM outer surface). The standoff distance was calculated to give a soil displacement of approximately 0.75 feet (1), which corresponds to 50 percent strain in the 18 inch thick ESM material systems.

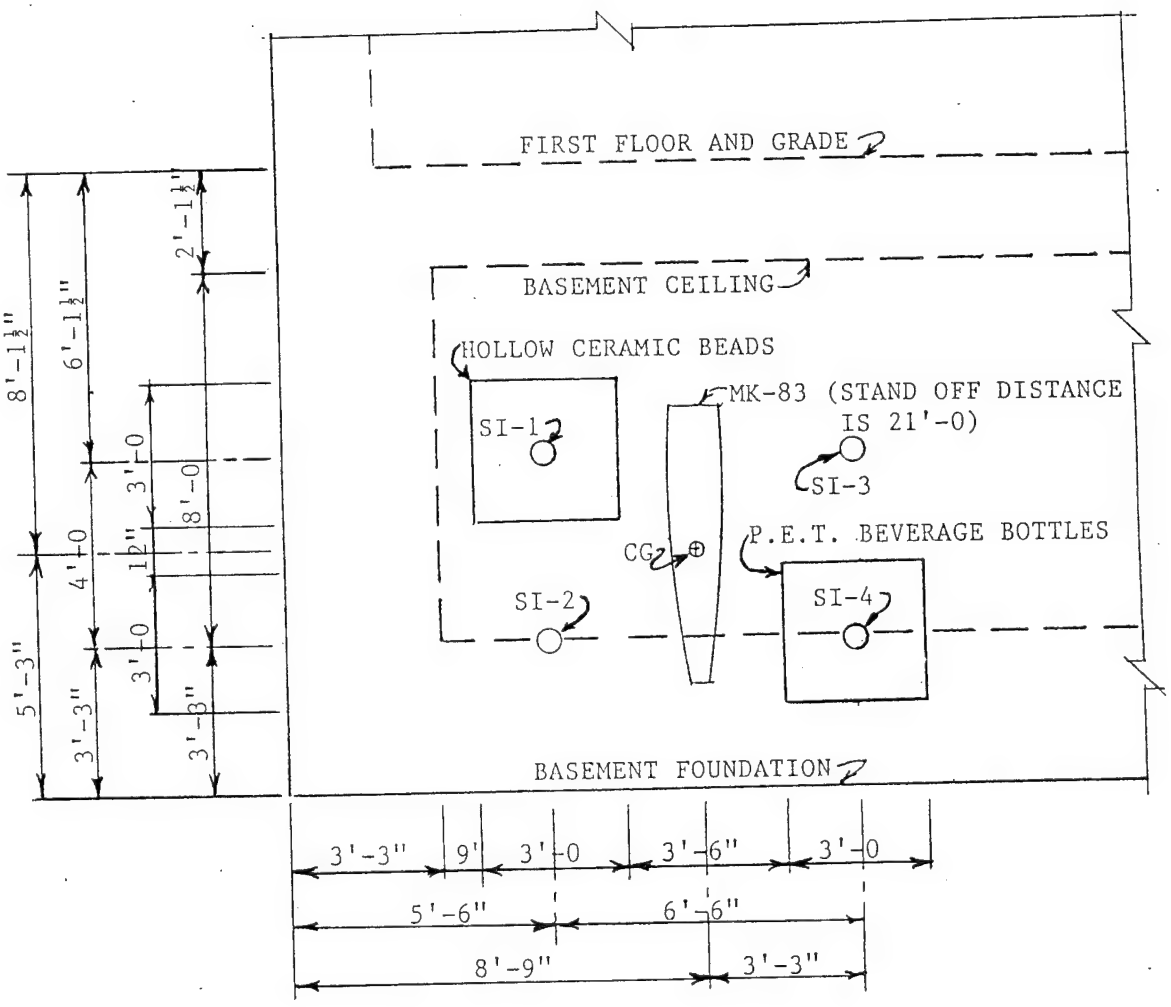

Figure 19. External Shock Mitigation Field Test Site Layout

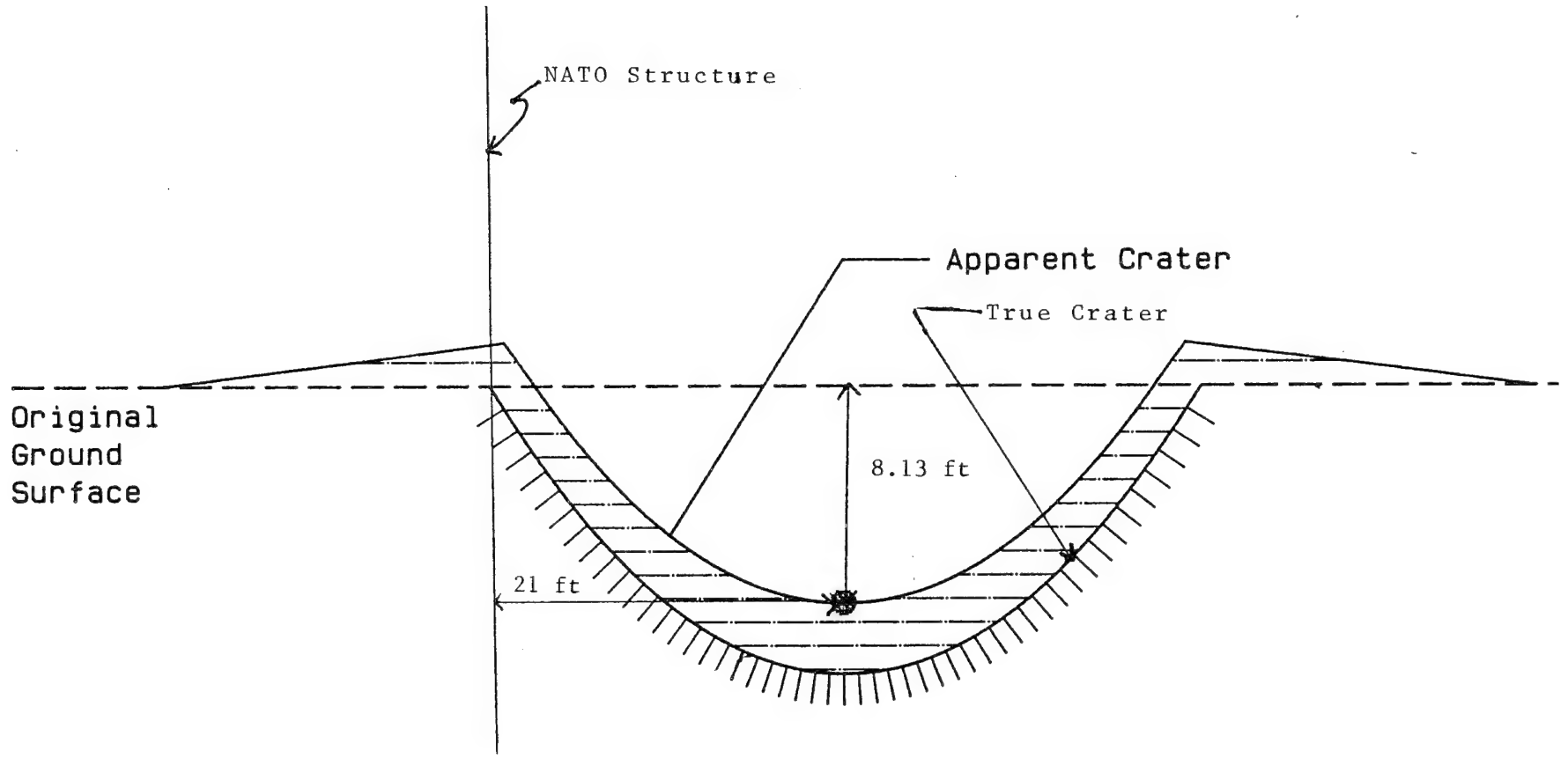

Figure 20. Crater Profile for 21 Foot Standoff at SKY-10

The following equation was used to calculate scaled peak free-field soil displacement:

$$d_o/W^{1/3} = f(500)(1/c)(R/W^{1/3})^{-n+1}$$

where:

$c = 600$ fps

$n = 3.25$

$f = 1.0$

$W = 526$ lbs

Seismic velocity, c = 600 fps for loose, dry, poorly graded sand was obtained from reference (1). This yields the following result for the standoff distance, R (ft):

$$R = \left[\frac{(1.0)(500)(526)^{1/3}}{(0.75)(600)}\right]^{1/2.25} \cdot (526)^{1/3} - 21.4$$

2. Materials

Figure 21 shows the cellular concrete, used as a binder for the polyester terephthalate (PET) beverage bottles, being poured from a small rotary mixer. Figure 22 shows the 3 by 3-foot by 18-inch deep mold used to preplace the PET bottles. The cellular grout was poured into the sealed mold, as shown in Figure 23, and infiltrated the interstices between the bottles. The finished mold, shown in Figure 24, was weighed, and based on the unit weight of the cellular concrete, the void volume (percent volume of air) was calculated as follows:

Total weight of the ESM material = 434 Lbs= W_{GS}

Total volume of ESM block = 13.5 ft^3 = V_T

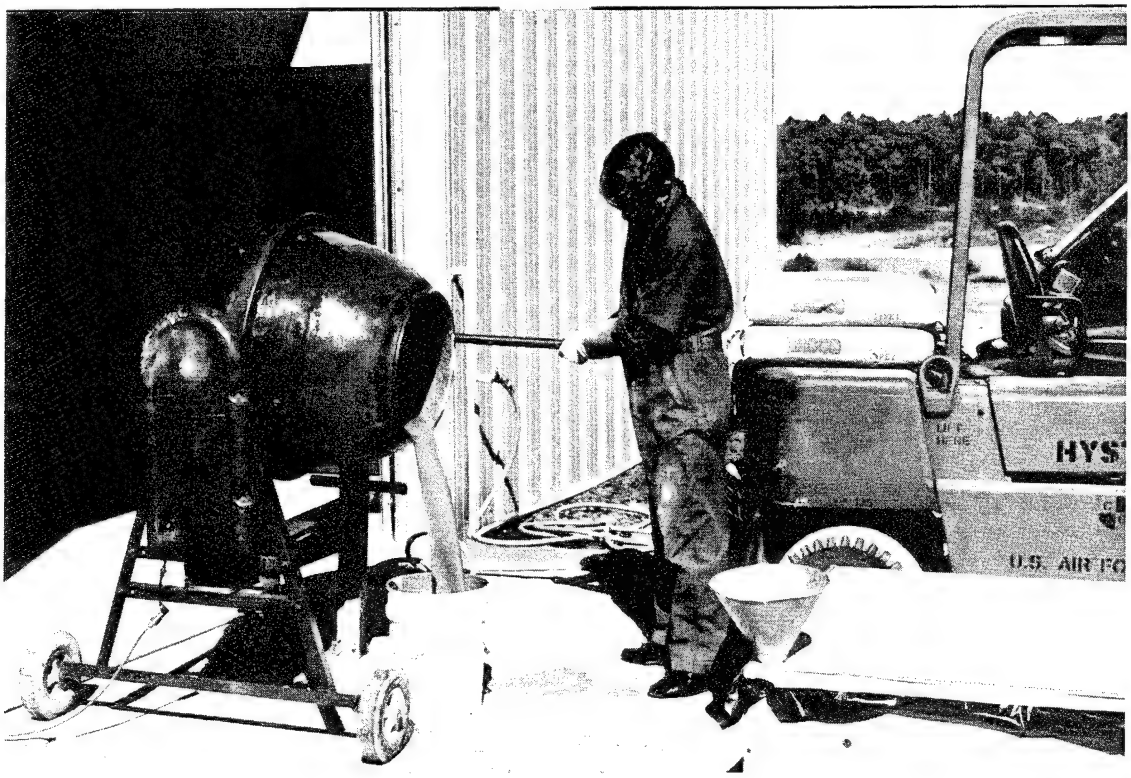

Figure 21. Mixing Cellular Grout

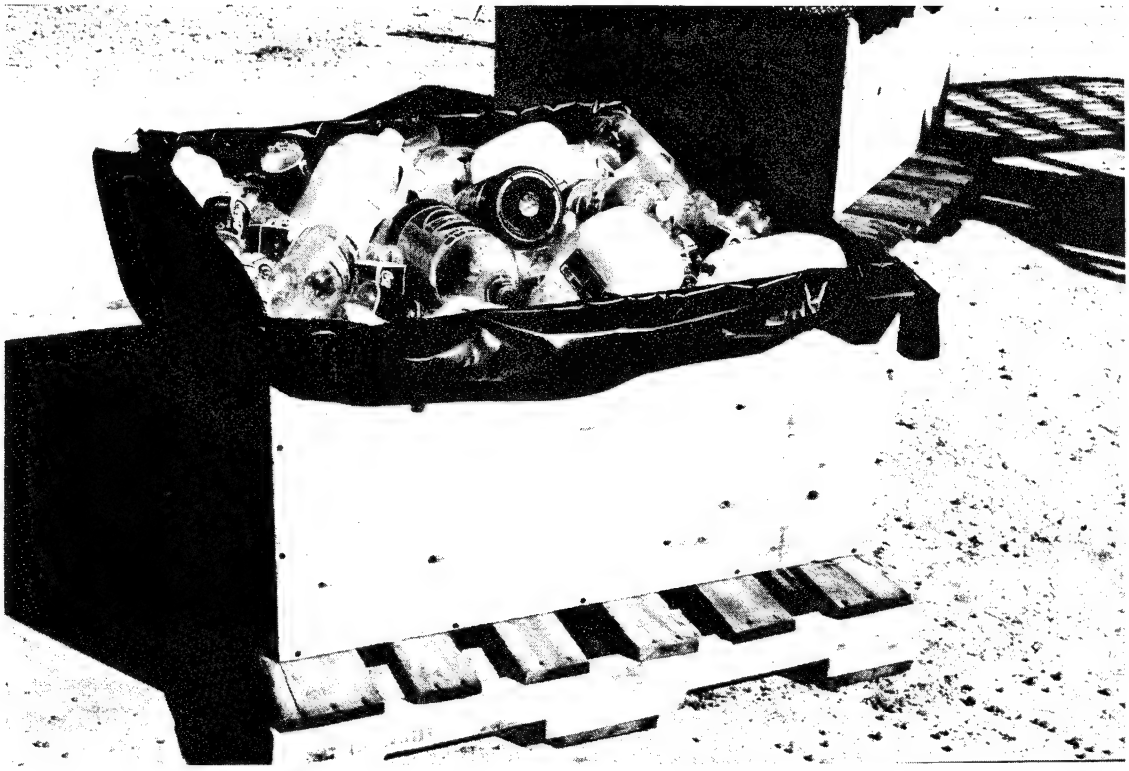

Figure 22. Three Foot Square by 18-Inch Deep Mold Containing Loose PET Bottles

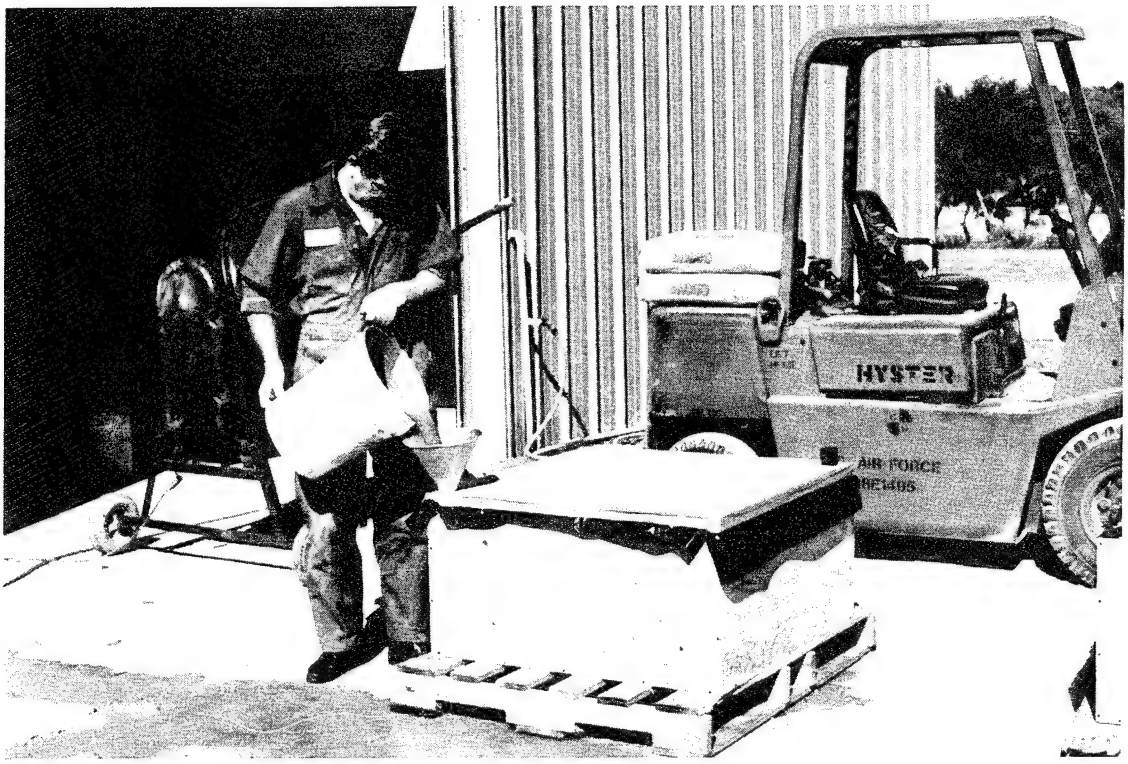

Figure 23. Pouring Cellular Grout

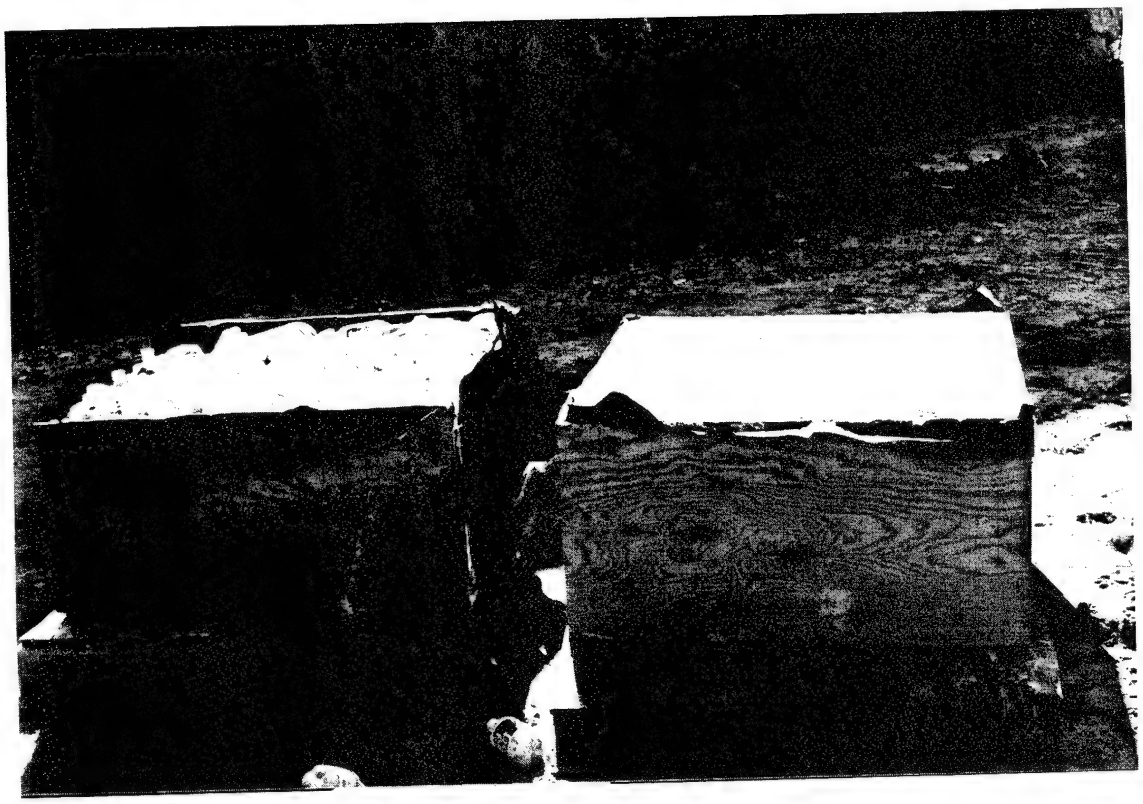

Figure 24. Completed Grouted PET Bottle Mold

Unit weight of cellular grout binder = 67 lbs/ft^3= ς_{CG}

$$\therefore \frac{V_{AB}}{V_T} = 1 - \frac{W_{GS}}{\varsigma_{CG} V_T} = 1 - \frac{434}{(67)(13.5)} = 0.52$$

Solid grout (not foamed) unit weight = 137 lbs/cubic foot= ς_{GS}

$$\therefore \frac{V_{AT}}{V_T} = 1 - \frac{W_{GS}}{\varsigma_{GS} V_T} = 1 - \frac{434}{(137)(13.5)} = 0.77$$

The hollow ceramic spheres, ranging in diameter from 5.7mm to 12.7mm and having a bulk density of 19 lbs/ft^3, were used to produce another potential ESM system. An epoxy binder was used to "glue" the beads together, and the composite material was poured into a mold of the same dimensions described above, as shown in Figure 25. The hollow spheres were premixed with 2 percent epoxy by weight prior to being introduced into the mold and cured overnight at room temperature. Based on the unit weight of the hollow spheres and the weight of the finished ESM material, the void volume (percent volume of air) was calculated as follows:

Total weight of the ESM block = 305 Lbs = W_T
Total volume of syntactic foam block= 13.5 ft^3= V_T
Unit weight of Epoxy binder = 64.5 lbs/ft^3 = ς_E
Unit weight of ceramic sphere solid material = 36 lbs/ft^3 = ς_{SS}

$$\frac{V_A}{V_T} = 1 - \frac{W_T}{1.02 V_T} * \left(\frac{1}{\varsigma_{SS}} + \frac{0.02}{\varsigma_E}\right) = 1 - \frac{305}{(1.02)(13.5)} * \left(\frac{1}{36} + \frac{0.02}{64.5}\right) = 0.38$$

C. EXPLOSIVE TEST

The north basement wall was excavated, and pressure gauges were attached to the wall at the appropriate locations relative to the center of gravity of the 1000 pound bomb, as shown in Figures 19 and 26. Figures 27 and 28 show placement of the GPET ESM system and the BHCS ESM system, respectively. The ESM material systems were then buried, and the soil compacted, as shown in Figure 29. Figures 30, 31, and 32 show placement of the bomb guide tube at the 21 foot standoff distance, and at a depth such that the bomb c.g. would be 8.13 feet below the ground surface. The 1000 pound bomb was armed, and subsequently lowered into place, as shown in Figures 33 and 34.

1. Results

The detonation created a crater approximately 45 feet in diameter and 15 feet deep, as shown in Figure 35. The BHCS and the GPET ESM systems were excavated and examined, as shown in Figures 36 and 37, respectively.

The BHCS ESM system sustained a permanent deformation of 9 to 10 inches, measured with a rule, as shown in Figure 38. The GPET ESM system sustained a permanent deformation of only 1 to 2 inches, measured with a rule, as shown in Figure 39. It appeared from the excavated samples that the GPET ESM system experienced about the same peak deformation as did the BHCS system, but decompressed and returned to almost its original size.

The pressure gauges located on the bare concrete basement wall, SI-2 and SI-3, recorded peak interface stresses of 1,150 psi and 548 psi, respectively. The theoretical interface pressure predicted by Conwep was about 490-500 psi. From the shape of the measured stress-time curve in Appendix A-2, it appears that gauge SI-2 malfunctioned, due to being contacted by a rock or bomb fragment. The transmitted stress recorded by gauge SI-1, centered behind the BHCS ESM system, recorded a peak stress of 52.3 psi, as shown in Figure 40. Gauge SI-4, centered behind the grouted PET ESM system, recorded a peak stress of 59.9 psi, as shown in Figure 41. The raw data from the pressure gauges are given in Appendix A.

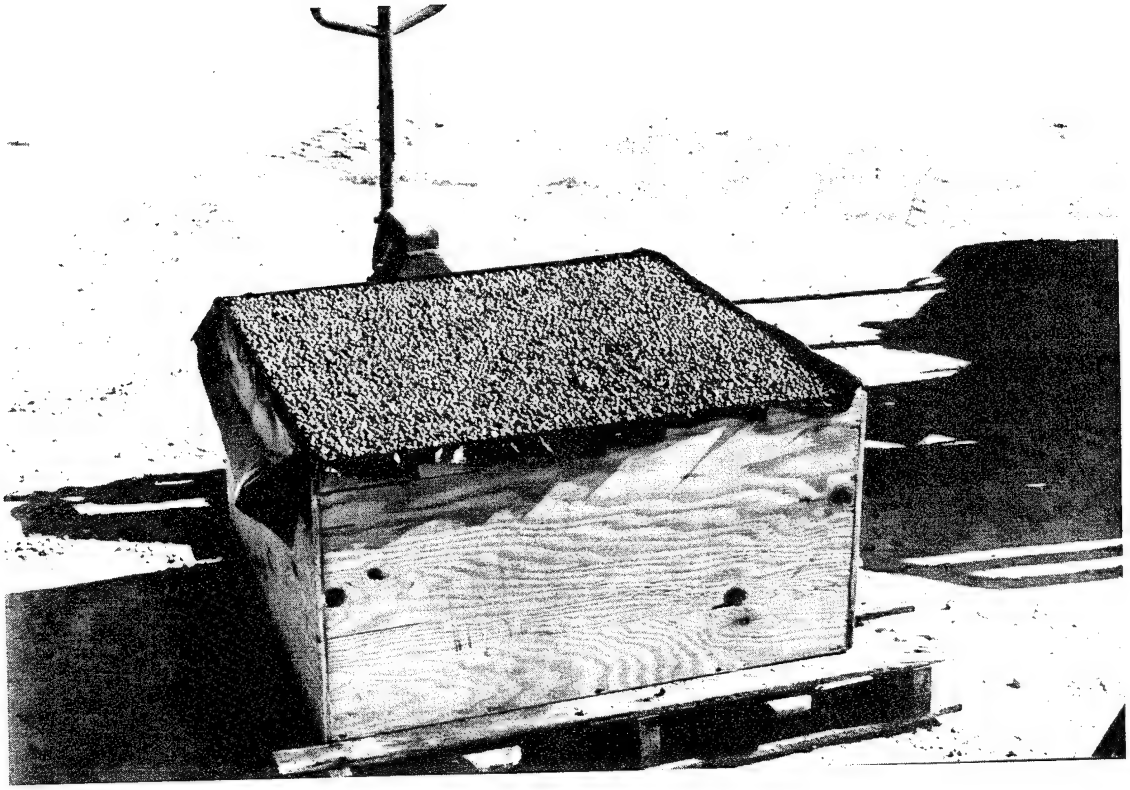

Figure 25. Completed Mold of Epoxy Bonded Hollow Ceramic Spheres

Figure 26. Installation of Pressure Gauges Into Basement Wall of NATO Structure

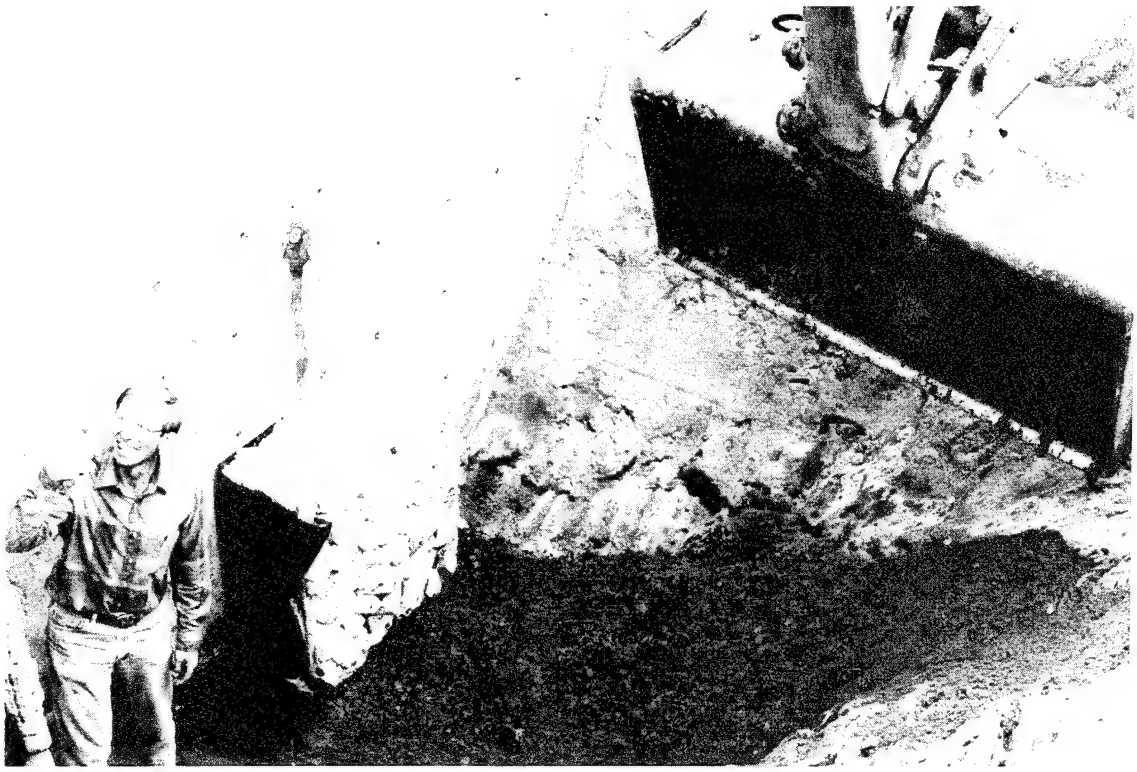

Figure 27. Placement of Grouted PET-ESM System Against Basement Wall

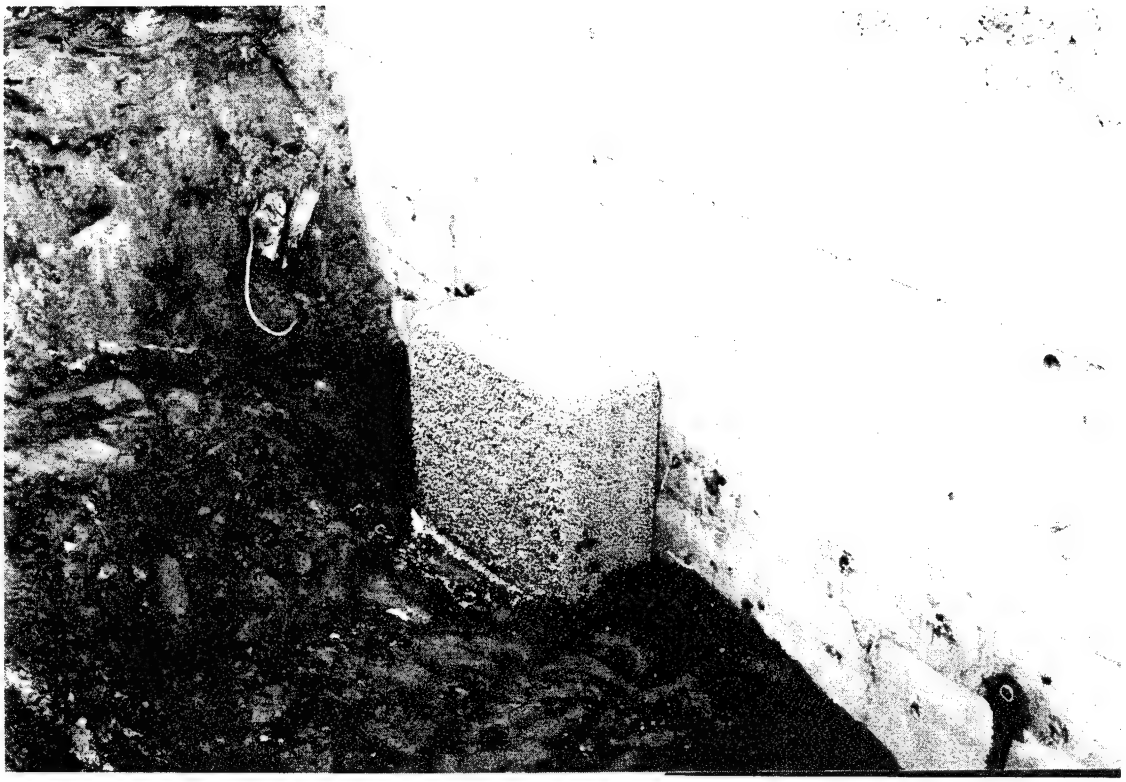

Figure 28. Placement of Bonded Hollow Ceramic Spheres-ESM System Against Basement Wall

Figure 29. Burial of ESM Systems

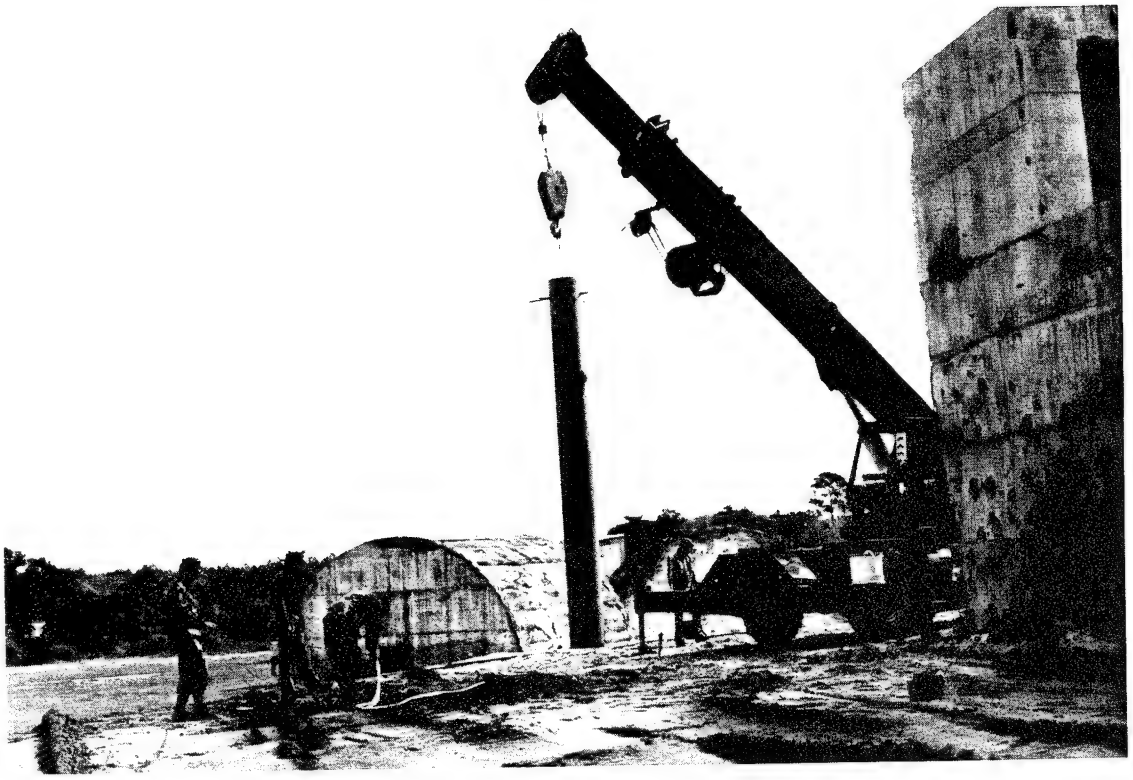

Figure 30. Positioning of Bomb Guide Tube in Excavated Hole

Figure 31. Placement of Bomb Guide Tube in Excavated Hole

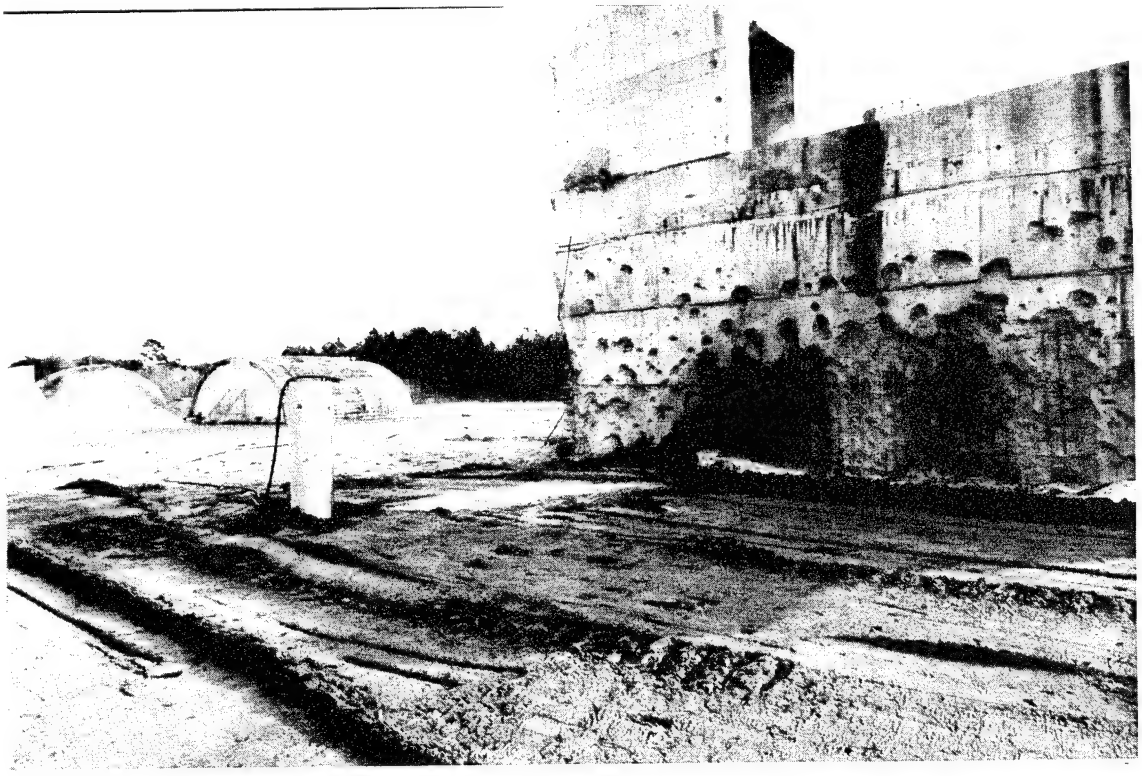

Figure 32. Burial of Bomb Guide Tube and Backfill Compaction

Figure 33. Arming the 1,000 Pound Bomb

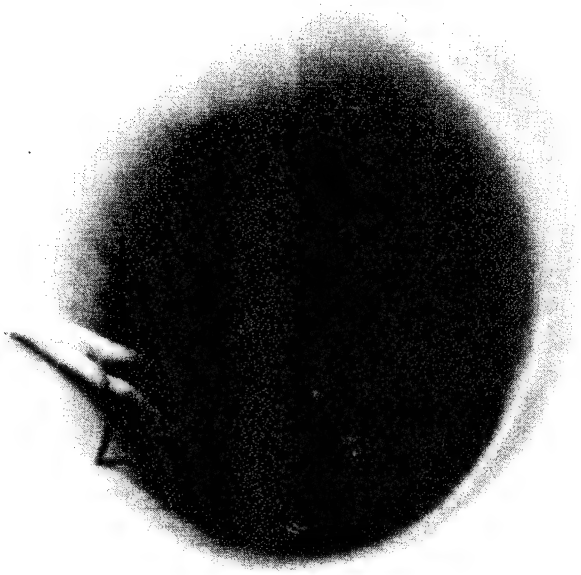

Figure 34. Lowering Bomb Into Hole

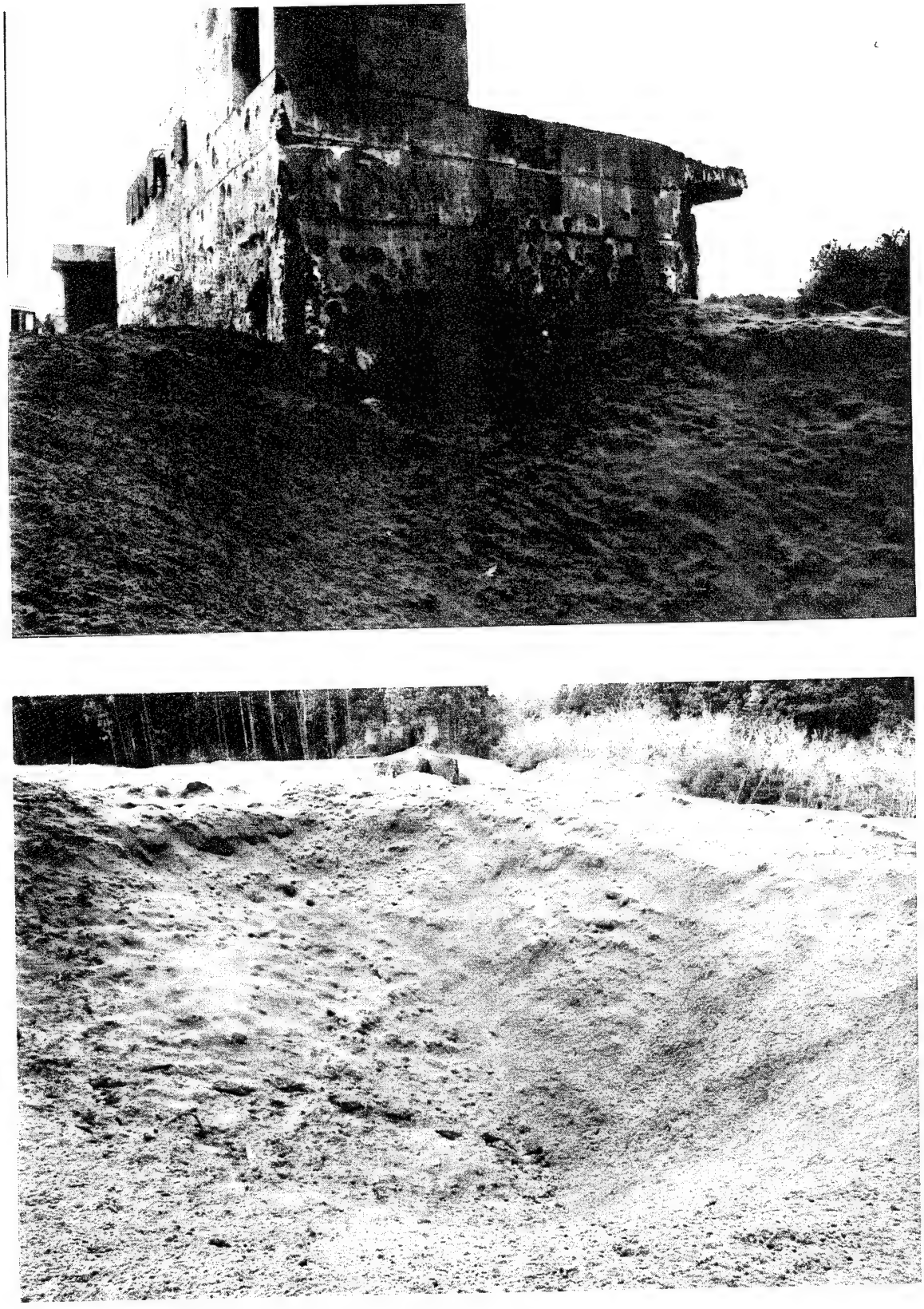

Figure 35. Resultant Crater Approximately 45 Feet in Diameter and 15 Feet Deep

Figure 36. Condition of BHCS-ESM System After Detonation

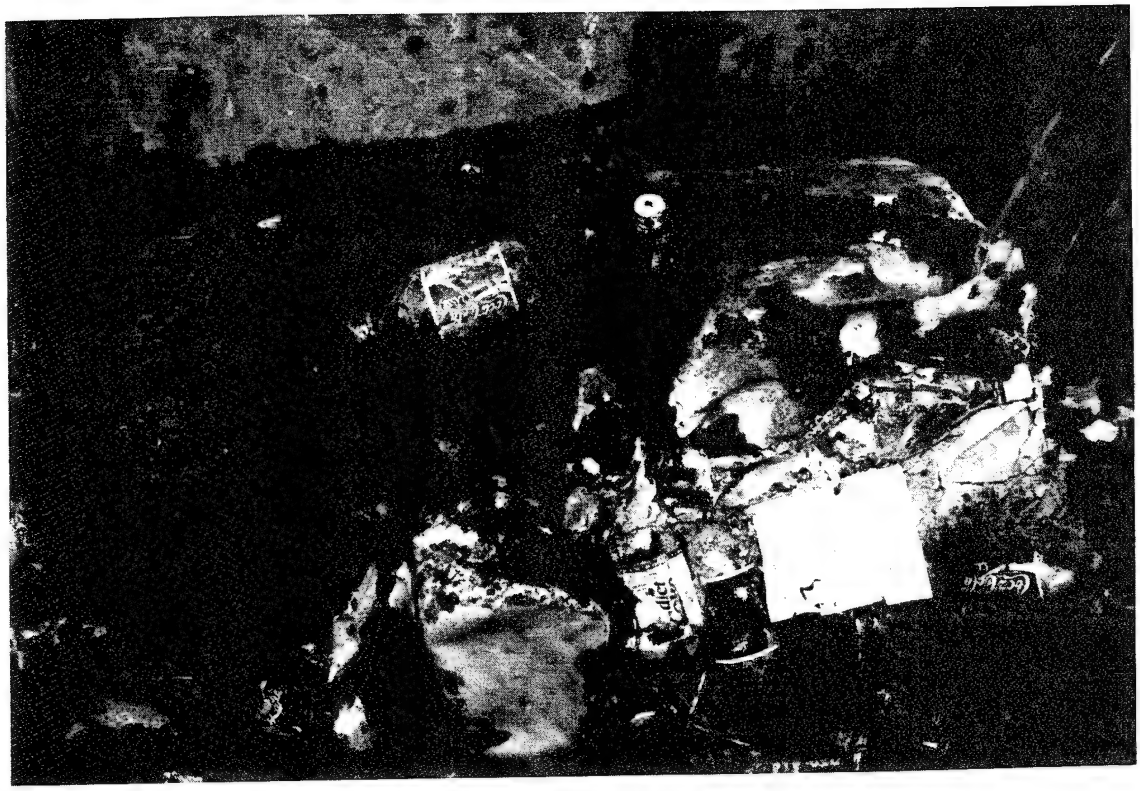

Figure 37. Condition of Grouted PET-ESM System After Detonation

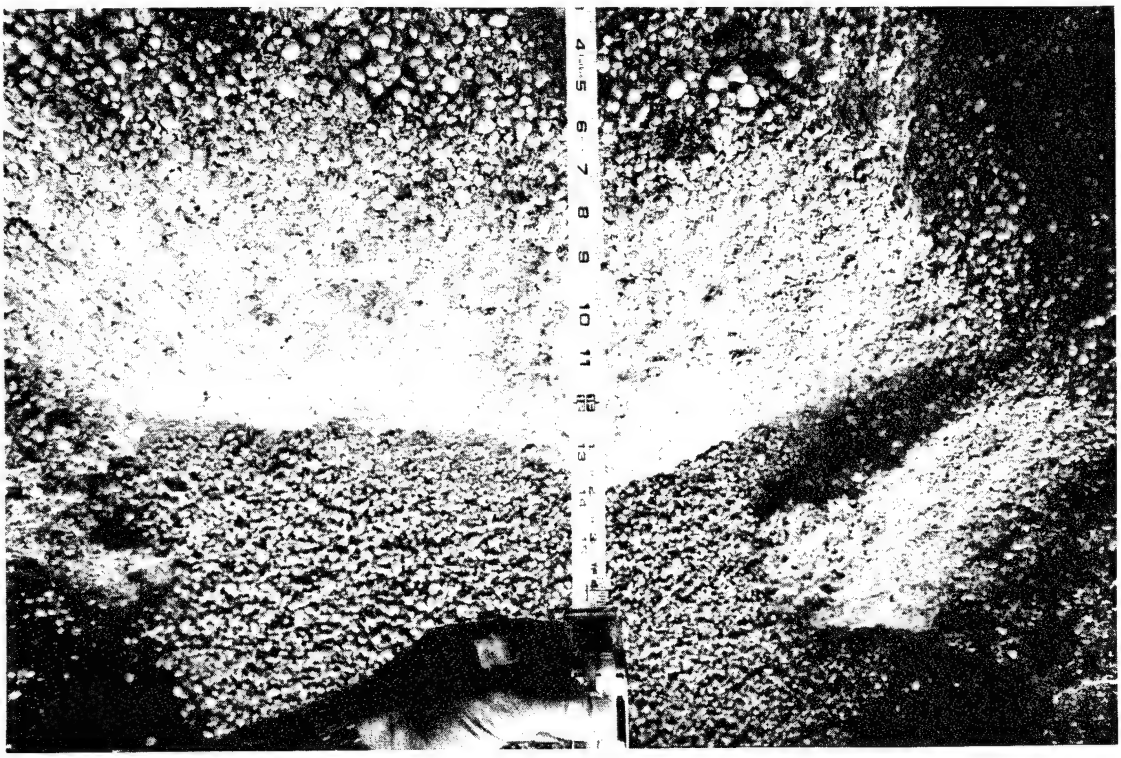

Figure 38. Thickness Remaining of BHCS-ESM Material System After Detonation

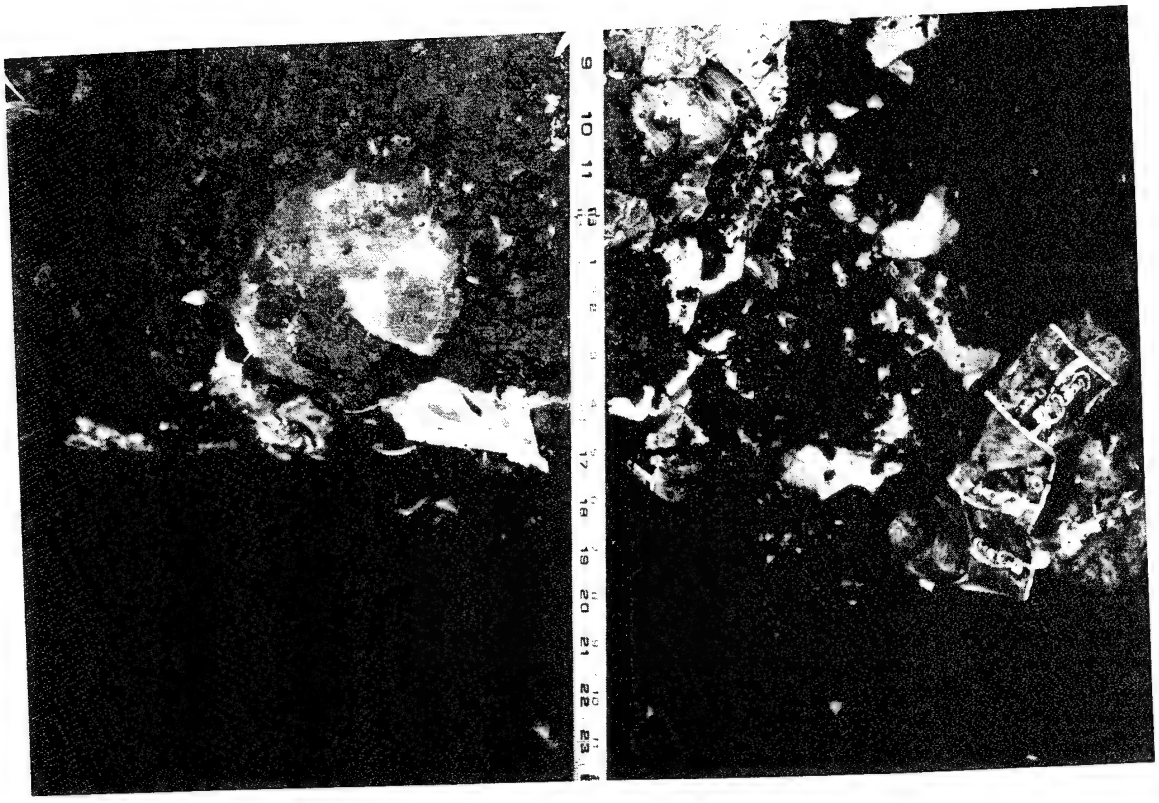

Figure 39. Thickness Remaining of Grouted PET-ESM Material System After Detonation

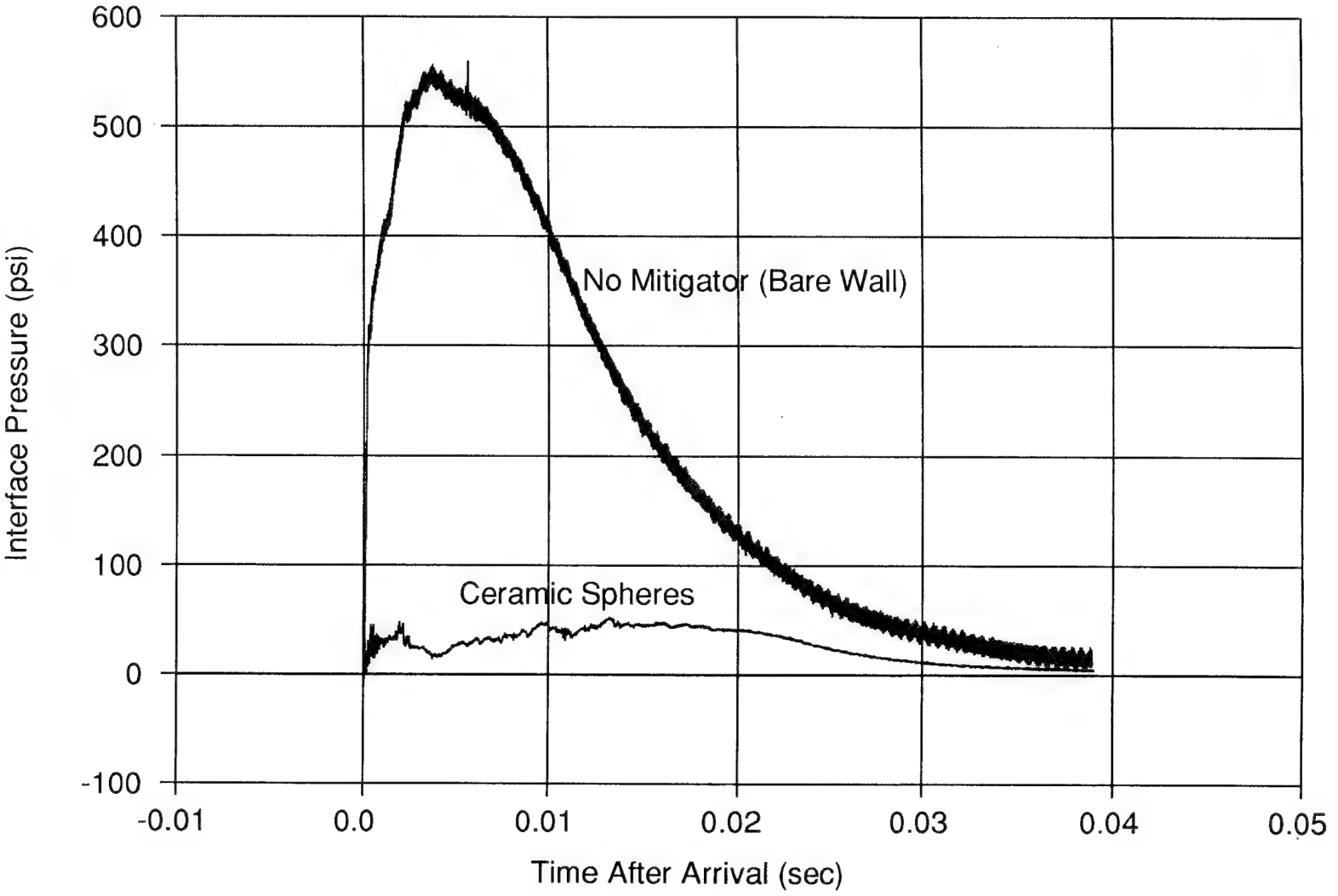

Figure 40. Interface Pressure for BHCS-ESM Material System Versus that for Bare Concrete Wall

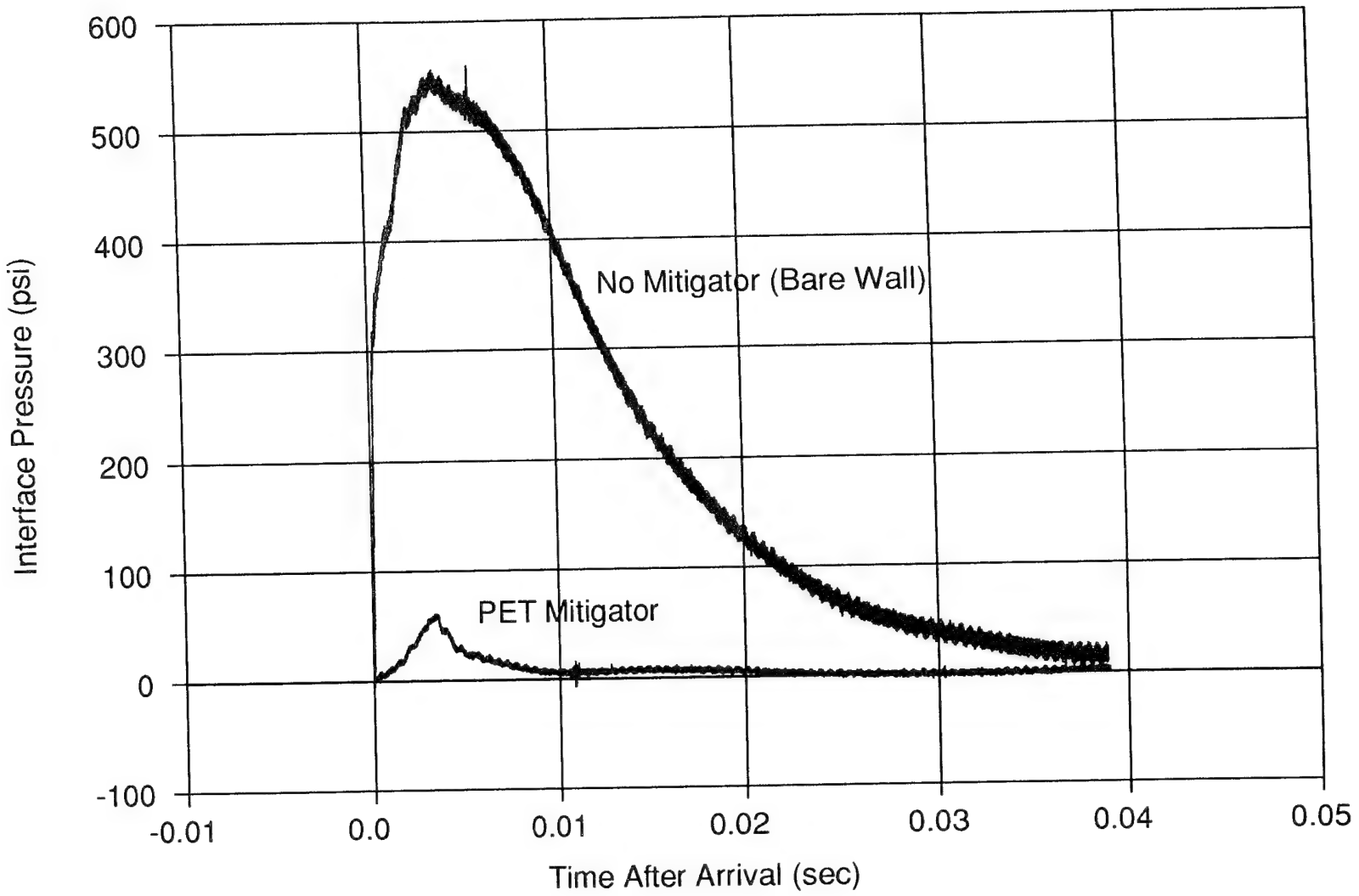

Figure 41. Interface Pressure for Grouted PET-ESM Material System Versus that for Bare Concrete Wall

2. Conclusions

The primary conclusions that can be reached from the field test are the following:

a. Both ESM systems appeared to have accommodated the backfill deformation without lockup, and transmitted only about 10 percent of the peak free field stress to the concrete basement wall.

b. The grouted PET ESM system (GPET) appears to be able to function as desired under multiple ground shock loadings. This is a first for ESM materials, which in the past have all deformed or crushed irreversibly.

c. The GPET ESM system attenuated 96.1 percent of the ground shock impulse as shown in Figure 42, calculated from the area under the P-T curves.

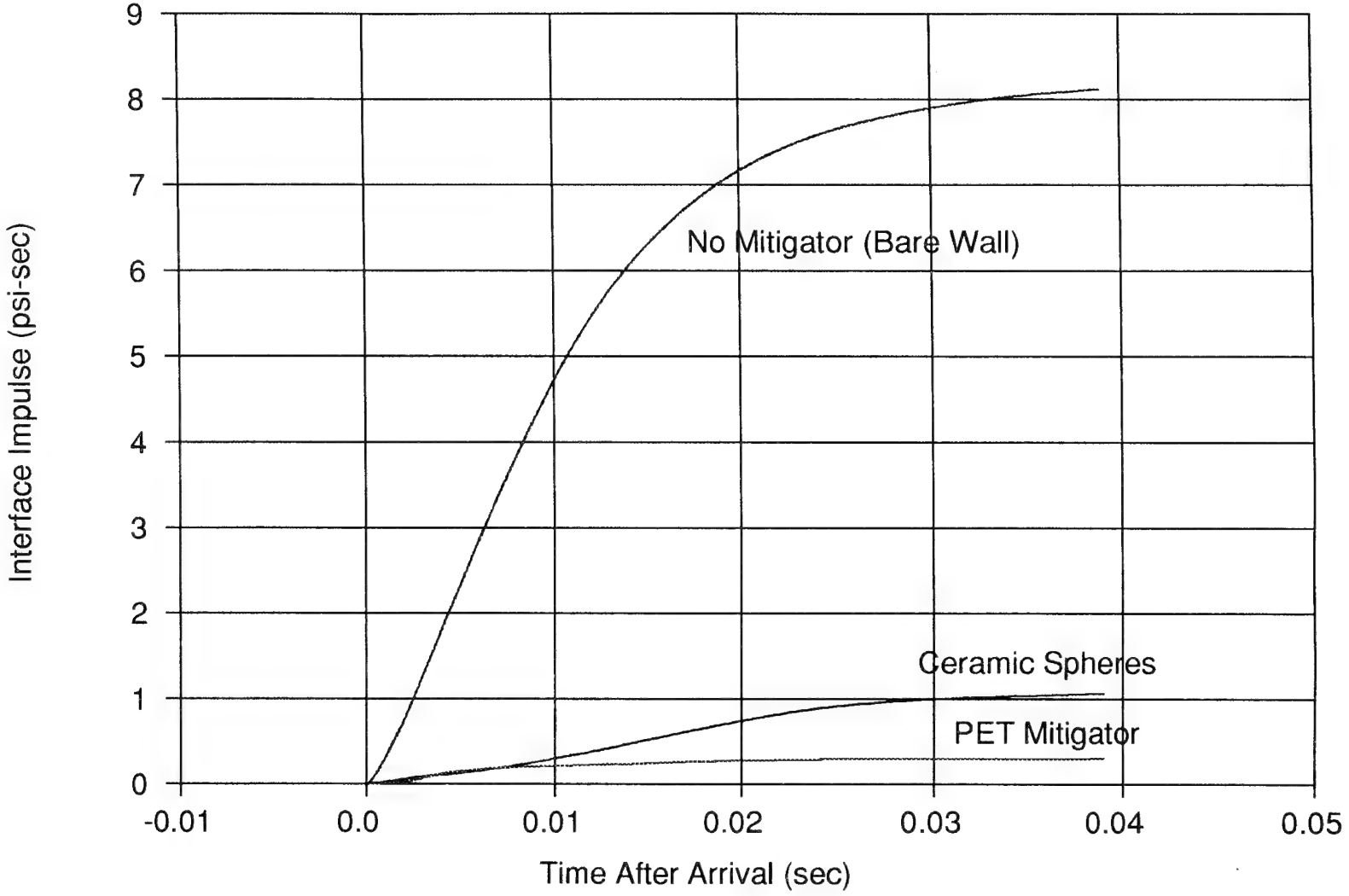

Figure 42. Comparison of Interface Impulse for Bare Concrete, the BHCS-ESM System, and the Grouted PET-ESM System

SECTION VI

ESM OPTIMIZATION

A. INTRODUCTION

The field test data from a close-proximity detonation of a conventional 1000-pound bomb against a below-grade wall of a protective structure illustrates the benefits of ESM materials. Figures 40, 41 and 42 illustrate the drastic reduction in both transmitted ground shock stress and transmitted ground shock impulse to a buried wall which can be achieved by using an ESM material.

B. ELASTO-PLASTIC BINDER

Figure 14 shows the unconfined compressive stress-strain curve of the cellular grout binder for the PET ESM System. This curve is very similar to the stress-strain behavior of an ideal plasto-elastic material, shown in Figure 1. Therefore, it was postulated that a binder-PET ESM material system would out perform the cellular grout binder system if the cellular grout binder were replaced by a binder that behaved more like an ideal elasto-plastic material. This material should have the performance characteristics described in Section IIIC.

Figure 43 illustrates the unconfined compressive stress-strain behavior of a low-density, closed-cell polyurethane foam binder. The polyurethane material used was Chempol 030-2334 resin and 030-2416 curing agent. This is a freon-blown, low-density foam having a unit weight of 1.3 lbs/ft^3. It was supplied by Cook Composites and Polymers, Kansas City, Missouri. Figure 43 also shows the stress-strain behavior for the same low-density, closed-cell polyurethane foam binder, incorporating the same volume percent of PET bottles. Calculating the total volume of air in this system by the method used in Section IV-B.2, the total volume of air was calculated to be 96 percent.

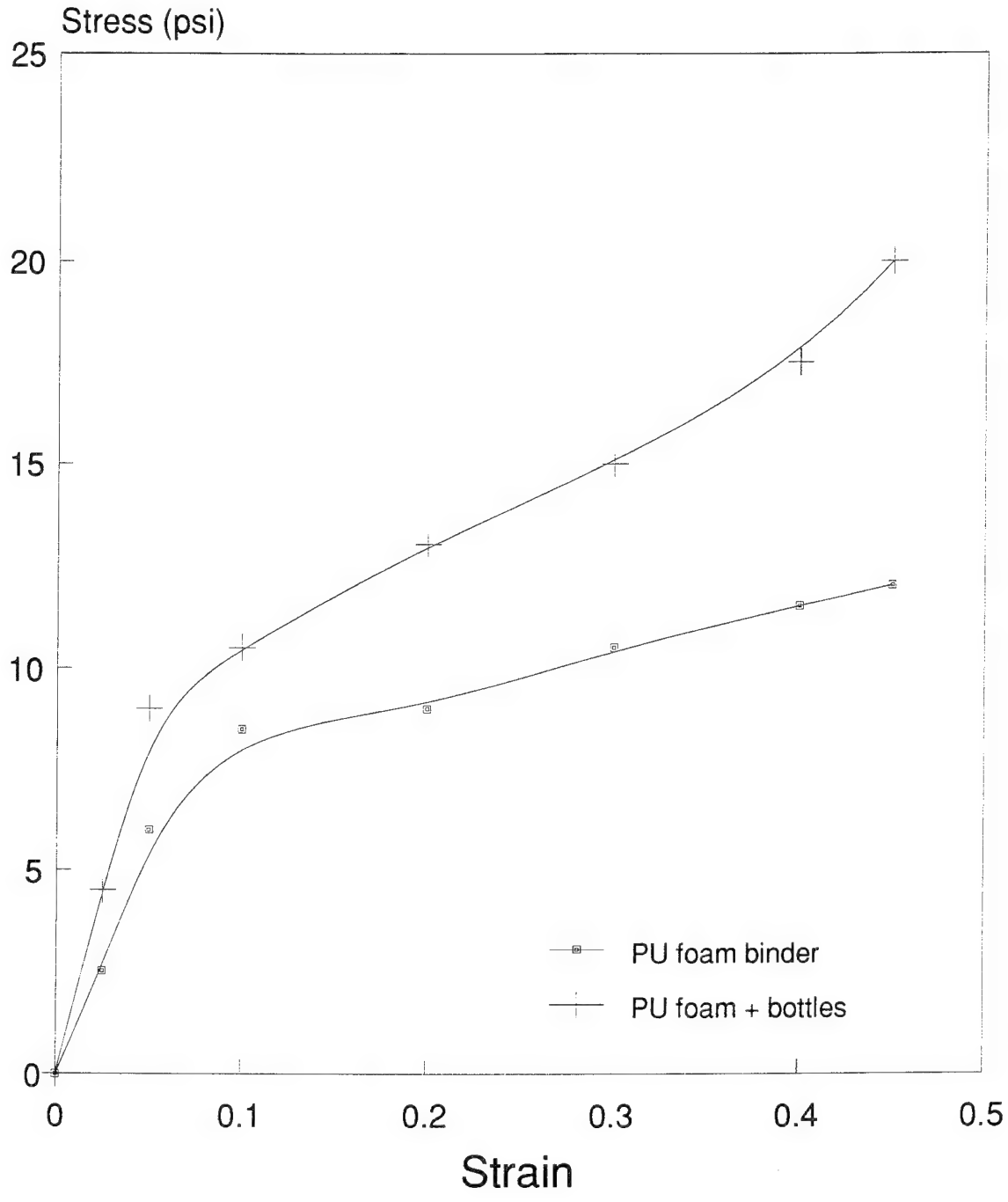

Figure 43. Comparison of Unconfined Compressive Stress-Strain Behavior of 1.3 lbs/ft^3 Neat Polyurethane Foam and Polyurethane Foam Plus PET Bottles

Both materials were tested in unconfined compression to 50 percent strain, which produced an interesting result. The low-density, closed cell polyurethane foam binder did not fully recover from the 50 percent deformation. In fact, only about 10 percent of the deformation was recovered, resulting in approximately 40 percent permanent deformation. However, the low-density, closed-cell polyurethane foam binder-PET (PUPET) bottle ESM material system recovered almost totally from the 50 percent deformation, resulting in a permanent deformation of approximately 7-8 percent.

C. QUASI-STATIC ADIABATIC PROCESS

When an ideal gas such as air, undergoes a quasi-static adiabatic process, the pressure, volume, and temperature changes are related by the following equations:

$$dQ = du + PdV = d(V + PV) - VdP$$
$$= C_v dT + PdV = C_p dT - VdP$$

Since dQ = 0 in an adiabatic process,

$$VdP = C_p dT$$
$$PdV = -C_v dT$$

Dividing elements of the first equation by corresponding elements of the second expression yields

$$\frac{dP}{P} = -\frac{C_p}{C_v}\left(\frac{dV}{V}\right) = -\varsigma \frac{dV}{V}$$

where ς is the ratio of the molar heat capacities, C_p/C_v. ς is constant in an adiabatic process involving small or moderate temperature changes, so that integration yields

$$\ln P = - \zeta \ln V + \ln(constant)$$

or,

$$PV^{\varsigma} = constant$$

The value of ς for air and other ideal gases can be obtained by measuring the speed of sound in the gas at a specific temperature. The computation of ς from sonic measurements is treated in standard thermodynamics texts (17).

In Figure 44, curve I represents the static, unconfined compressive stress-strain curve of the PUPET system. Curve II represents the quasi-static adiabatic compression of air trapped in the PET bottles. Comparison of curve II with curve I shows that the two curves become parallel, and therefore the adiabatic compression of air in the PUPET system starts when the polyurethane foam binder reaches its yield point. Upon releasing the load at 50 percent strain or more, adiabatic expansion of the air in the bottles occurs, and the PUPET system returns to its original size and shape, as shown in Figures 45 and 46.

D. CONCLUSION

It would be advantageous to use the PUPET ESM material system, rather than the GPET ESM material system, to resist repeated deformations from multiple ground shock loadings.

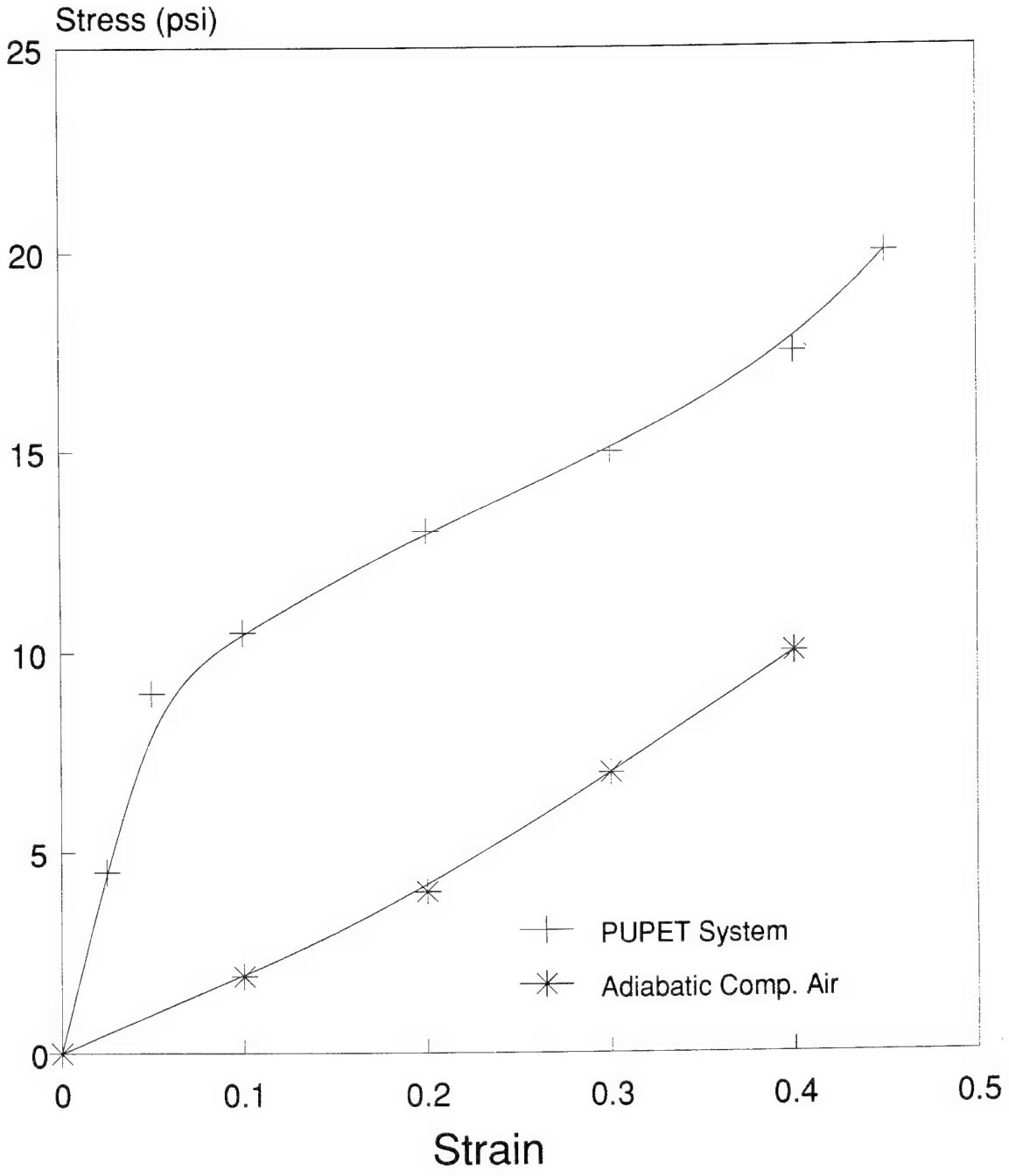

Figure 44. Stress-Strain Behavior of Polyurethane Foam-PET Bottle System Compared with the Adiabatic Compression of Air

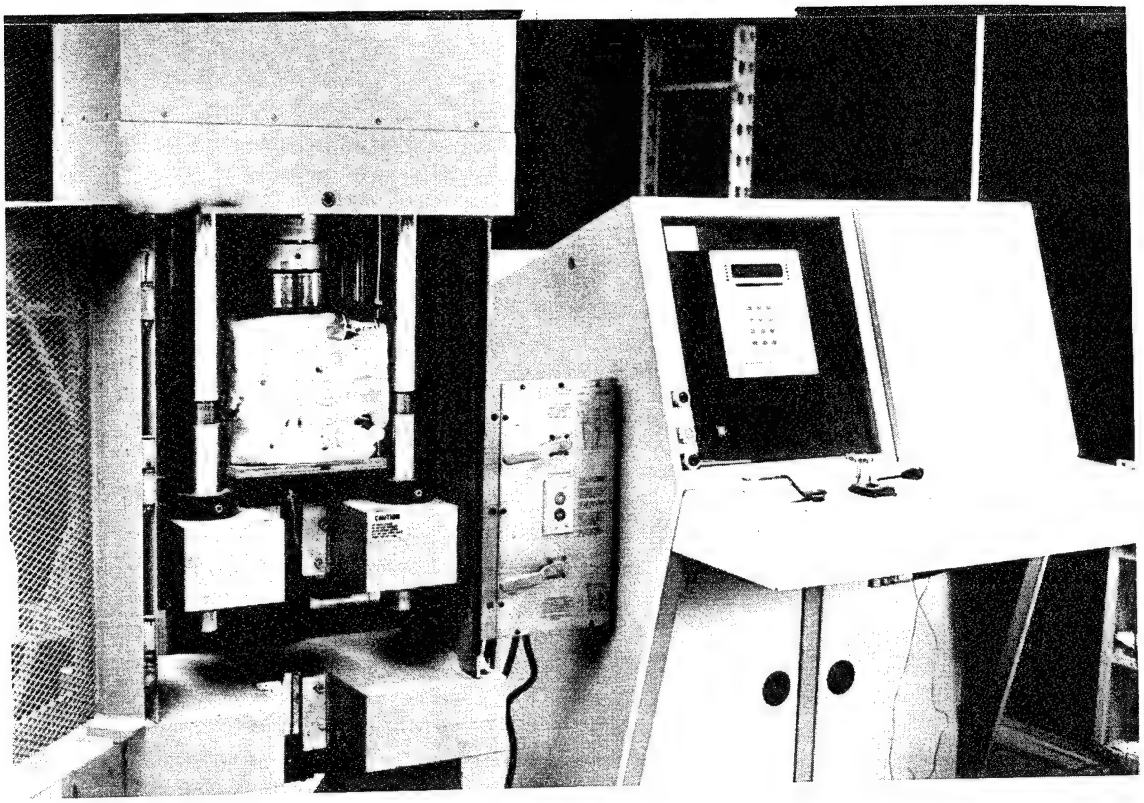

Figure 45. Polyurethane Foam Binder-PET ESM Material System in Test Frame

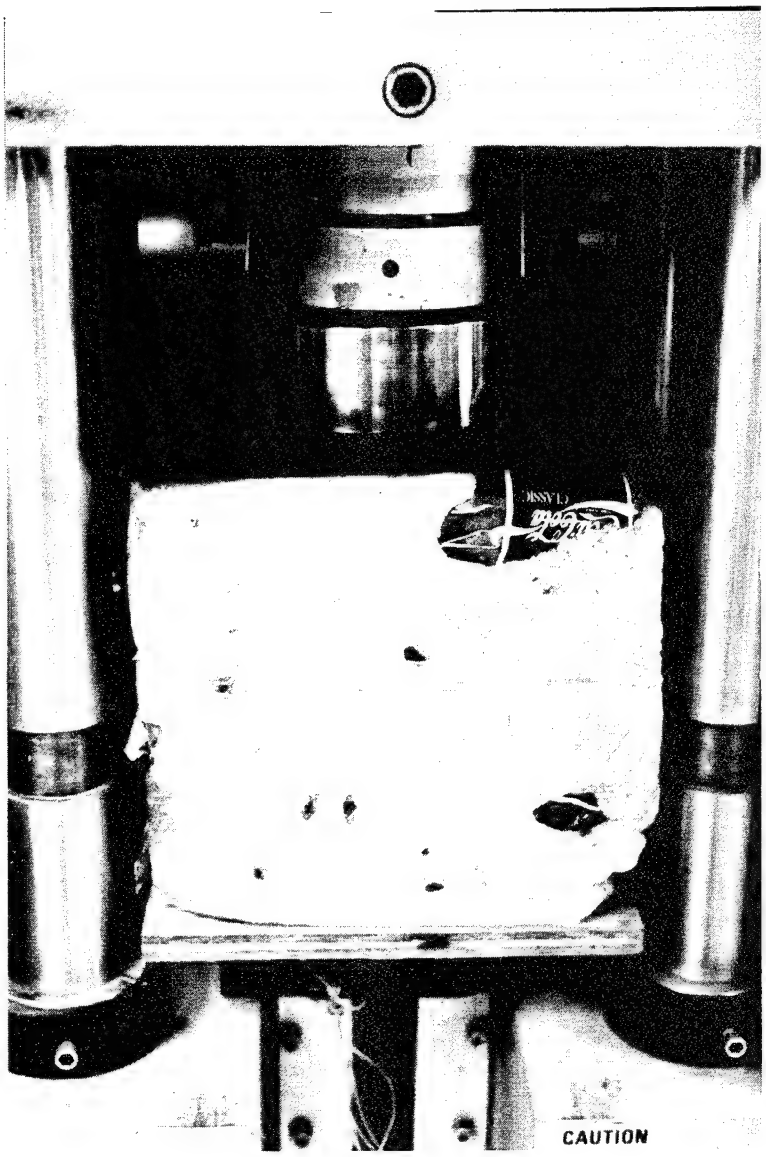

Figure 46. Polyurethane Foam Binder-PET ESM Material System Recovery After 50 Percent Deformation.

SECTION VII

CONCLUSIONS AND RECOMMENDATIONS

A. CONCLUSIONS

This work produced a very efficient ESM material system, composed of virgin or possibly recycled plastic PET containers, in a matrix consisting of a low-density foam system. Field testing demonstrated the utility of this ESM system, which transmitted only 10 percent of the peak ground shock stress, and attenuated 96.1 percent of the ground shock impulse. Further laboratory work demonstrated that using a low-density, closed-cell polyurethane foam as the binder of the "PET plastic bottle" system will enable the ESM material to accommodate multiple ground shock events, whereas previous ESM material systems employed single-use, crushable material systems.

B. RECOMMENDATIONS

Further ground shock testing should be performed on optimized, low-density, closed-cell, polyurethane foam-PET bottle (PUPET) ESM designs, using multiple ground shock events at the Tyndall AFB Sky-10 test facility.

SECTION VIII

REFERENCES

1. Drake, J.L., et.al., Protective Construction Design Manual: "Groundshock and Cratering" (Section V), Final Report, ESL-TR-87-57, Air Force Civil Engineering Support Ageny, Tyndall Air Force Base, November 1989.

2. Engineering Research Associates, Bureau of Mines, and the Armour Research Foundation, Underground Explosion Test Program, Volume 2, "Rock", Contract No. DA-04-167-ENG-374, San Antonio, Texas, May 1964.

3. Vaile, R. B., Isolation of Structures from Ground Shock, Operation PLUMBOB, WT-1424, Stanford Research Institute, Menlo Park, California, 1957.

4. Sevin, Eugene, Ground Shock Isolation of Buried Structures, Armour Research Foundation of Illinois Institute of Technology, Report No. AFSWC-TR-59-47, Contract No. AF-29(601)-1134 for Air Force Special Weapons Center, Kirtland Air Force Base, New Mexico, August 1959.

5. Sevin, E., Shenkman, S. and Welch, E., Ground Shock Isolation of Buried Structures, Armour Research Foundation of Illinois Institute of Technology, Report No. AFSWC-TR-61-51, Final Report, Contract No. AF-29(601)-2586 for Air Force Special Weapons Center, Kirtland Air Force Base, New Mexico, July 1961.

6. Da Deppo D.A., and Werner J.F., The Influence of Mechanical Shielding on the Response of a Buried Cylinder, Engineering Research Laboratory, University of Arizona, Tucson, Arizona, February 1962.

7. Fowles, G.R., and Curran D.R., Experimental Testing of Shock Attenuating Materials, Final Report, AFSWC-TDR-62-22, Poulter Laboratories, Stanford Research Institute, Menlo Park, California, March 1962.

8. Smith, E.F., and Thompson, J.N., A Study of Vermiculite Concrete as a Shock-Isolating Material, Structural Mechanics Research Laboratory, The University of Texas, Contract Report No. 6-83 for U.S. Army Engineer Waterways Experiment Station, Vicksburg, Mississippi, under Contract No. DA-22-079-ENG-342, October 1963.

9. Hoff, George C., "Shock-Isolating Backpacking Materials, A Review of the State of the Art," Proceedings of the Soil-Structure Interaction Symposium, University of Arizona, Tucson, Arizona, June 1964.

10. Klotz, L.H., Evaluation of Tunnel Liners in Granite, Shot HARDHAT, Operation NOUGAT, Static Stress-Strain curves for Various Materials Investigated for Use as Packing, University of Illinois, Final Report, Vol. III, Contract No. AF-29(601)-4993 for the Air Force Weapons Laboratory, Kirtland Air Force Base, New Mexico, February 1964.

11. Rempel, J.R., Shock-Wave Attenuation in Elastic Rigid Foams, Poulter Laboratories, Stanford Research Institute, Contract No. AF-29(601)-4363 for Air Force Weapons Laboratory, Kirtland Air Force Base, New Mexico, October 1963.

12. Hoff, George C., "Energy Dissipating Characteristics of Lightweight Cellular Concrete," Journal of the Mississippi State University, State College, Mississippi, 1963, pp. 195-196.

13. Hoff, George C., Shock Absorbing Concrete, Defense Atomic Support Agency, Washington D.C., by the U.S. Army Engineer Waterways Experiment Station, Vicksburg, Mississippi.

14. Hinckley, W.H. and Yang, J.C.S., Analysis of Rigid Polyurethane Foam as a Shock Mitigator, Naval Ordnance Laboratory, NOLTR 73-162, Silver Spring, Maryland, August 1973.

15. Denson, R.H., Ledbetter, W.B., and Saylak, D., Six Candidate Shock Attenuating Material Systems for the Alternate National Military Command Center Improvement Project-Omaha District, Final Report SL-82-17 Prepared for the U.S. Army Engineer District, Omaha, Nebraska, September 1982.

16. Ross, C.A., Split-Hopkinson Pressure Bar Tests, Final Report, ESL-TR-88-82, Air Force Engineering and Services Laboratory, Tyndall Air Force Base, March, 1989.

17. Zemansky, M.W. and Van Ness, H.C., Basic Engineering Thermodynamics, McGraw-Hill Book Company, 1966, pp.103.

APPENDIX A

FIELD TEST DATA

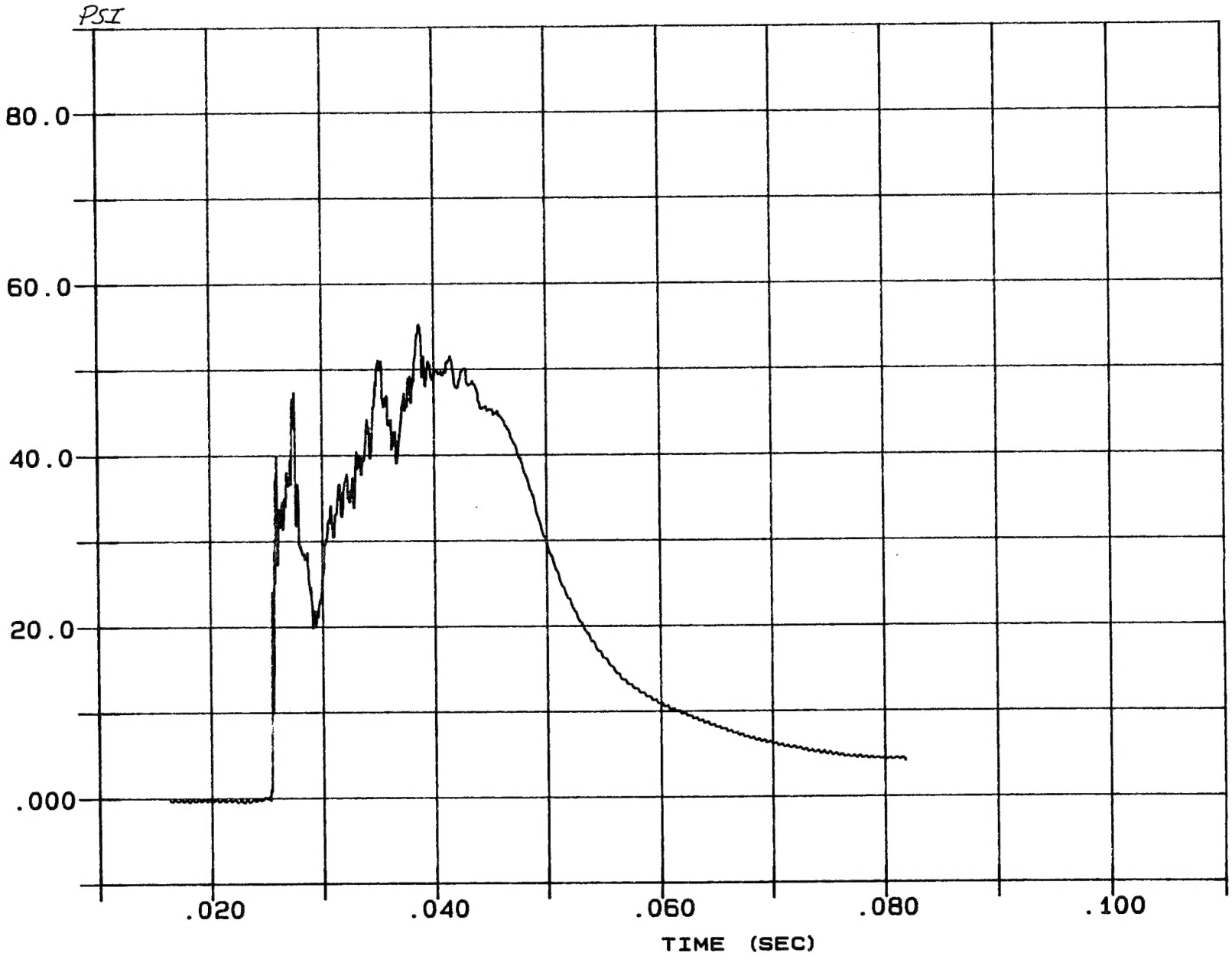

Figure A-1. Results from Soil Interface Gauge SI-1

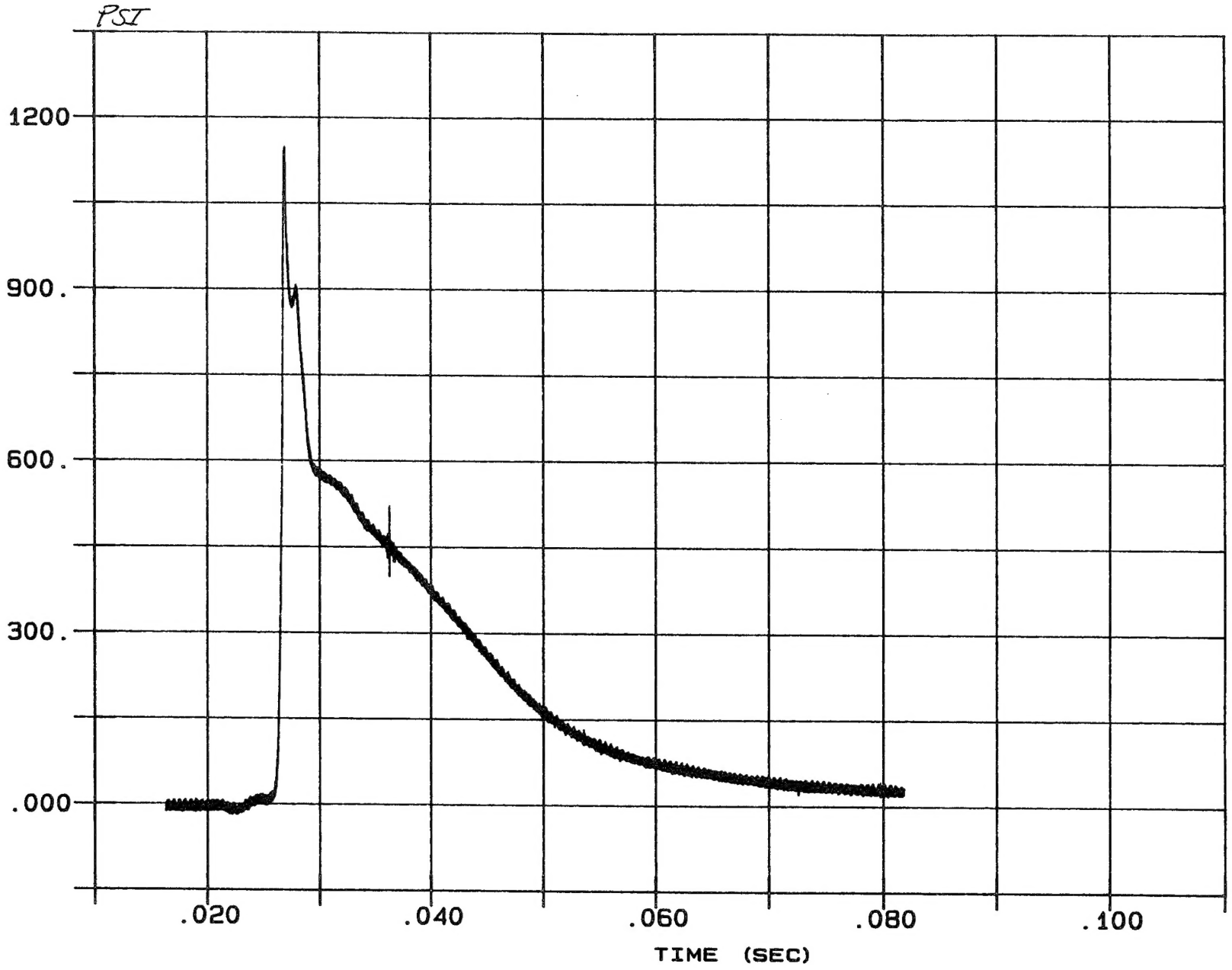

Figure A-2. Results from Soil Interface Gauge SI-2

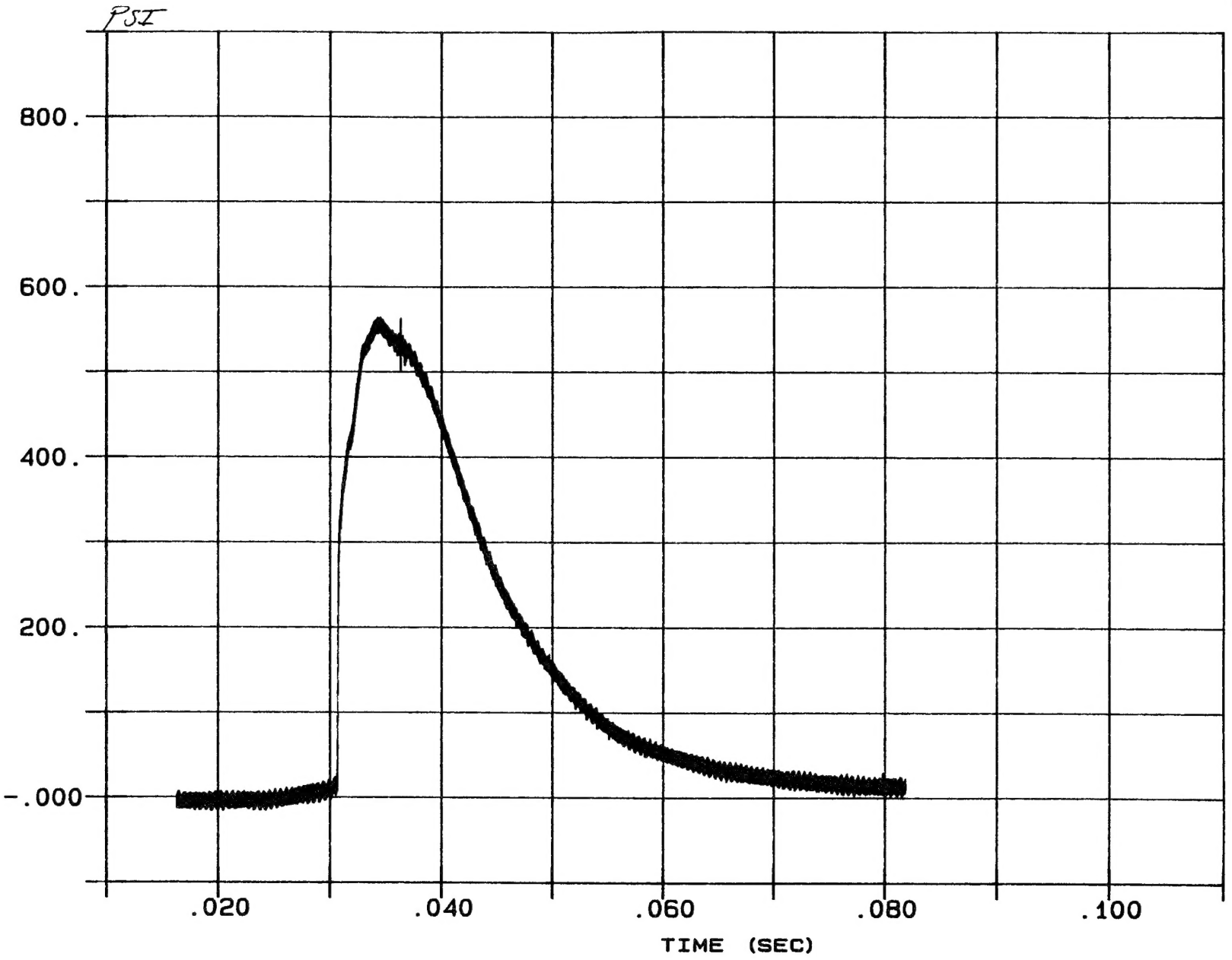

Figure A-3. Results from Soil Interface Gauge SI-3

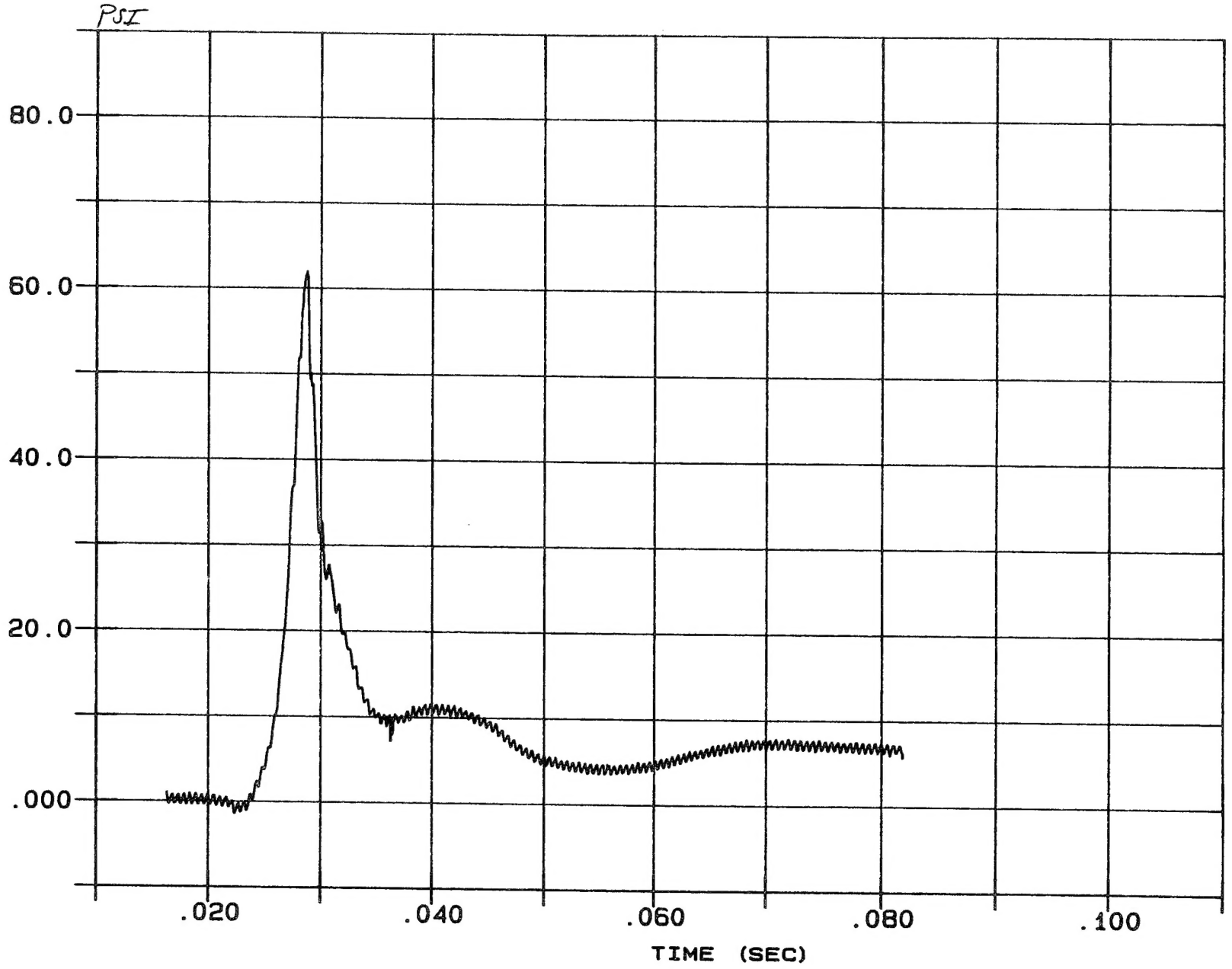

Figure A-4. Results from Soil Interface Gauge SI-4